Reactivity and selectivity in glycosylation reactions

Vorm, S. van der

Chapter 8

Stereoselectivity of C-2- and C-5-modified furanosides: a computational and experimental study

Introduction

Of the many structurally different carbohydrates, furanosides, the five-membered ring carbohydrates, are common components of plant- and bacterial oligosaccharides, and form the basis of DNA/RNA as nucleotides.[1–7] Glycosylation reactions with furanosides proceed with much the same chemistry as six-membered ring pyranosides. The glycosylation mechanism therefore proceeds through a pathway having S_N1-like and S_N2-like character. Furanosides are typically more reactive than pyranosides because they have one electron-withdrawing oxygen substituent less, and they are conformationally more flexible and can easier accommodate the double bond character upon oxocarbenium ion formation in the ring. In this chapter the stereoselectivity of S_N1-type glycosylations are investigated for furanosides, bearing different ring substituents. The stereoelectronic effects brought about by fluorine, azide, or the benzyloxy groups on C-2 and a methyl uronate or benzyloxymethyl group at C-5 are probed, as these can have tremendous influence on both the reactivity and the stereoselectivity of the glycosylation

reaction. The stereochemical outcome of experimental glycosylations of the differently functionalized furanosides is interpreted using computational analysis of the stability of the reactive intermediates in the dissociative mechanism, the furanosyl oxocarbenium ion.

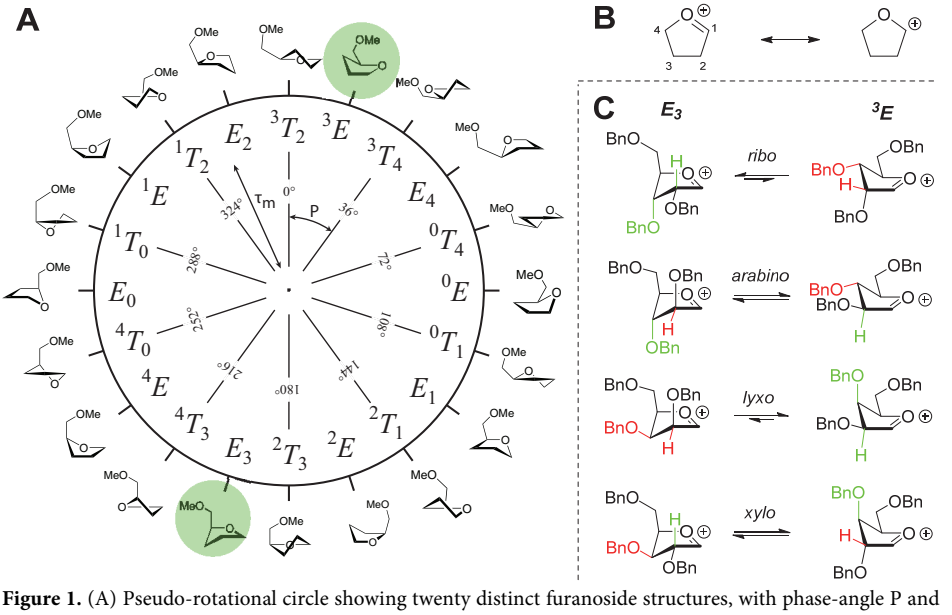

Figure 1. (A) Pseudo-rotational circle showing twenty distinct furanoside structures, with phase-angle P and puckering amplitude τ_m.[8] Green circles indicate the two major conformations of oxocarbenium ions. (B) Two resonance structures of a cyclic furanosyl oxocarbenium ion. (C) The two principal conformations of the two-conformer model (E_3-^3E) shown for every carbohydrate configuration, example taken as their tri-*O*-benzyl protected form. Colors indicate relative preferential orientations for H-2 and O-3 (see Chapter 1), green is relatively stabilizing whereas red is relatively destabilizing.

Furanosides readily attain different conformations, and all the different possible geometric shapes a five-membered ring can adopt can be described by a pseudo-rotational circle (Figure 1A).[9,10] The phase angle (P) defines the conformation of the ring, and the puckering amplitude (τ_m) describes the amount of distortion from the median plane the outlying atoms have.[8,11] In the middle of this circle, all five ring atoms are in the same plane, and all the substituents suffer from eclipsing interactions. Each furanoside, neutral or charged, has its own preferential conformation or suite of conformations, depending on the nature of the ring substituents and their orientation.

The conformations adopted by the reactive intermediates in S_N1-type substitutions, the oxocarbenium ions, are limited to a smaller region of the pseudo-rotational circle.[12] The oxocarbenium ion has two extreme resonance structures (Figure 1B), the most stable of the two features a C=O double bond which places four of the five

ring atoms in the same plane. The remaining ring-atom, C-3, will be out of the oxocarbenium ion plane, to minimize eclipsing interactions of its substituents. Therefore, the two most likely structures of an oxocarbenium ion will be the E_3 and ^3E conformations, or conformations closely related to those. The orientational preferences of each substituent in these two conformations has been investigated by the group of Woerpel (see also Chapter 1), the results of which are graphically displayed in Figure 1C.[13–17] The substituent on C-2 is preferentially placed in a sterically less demanding *pseudo*-equatorial orientation, simultaneously allowing the *pseudo*-axially orientated C–H bond to be aligned for hyperconjugative stabilization ($\sigma \rightarrow p/\pi^*$) of the anomeric carbocation. The substituent on C-3, on the other hand, is preferentially placed in a *pseudo*-axial orientation, as this brings the electron density of the electronegative oxygen atom closer to the oxocarbenium ion than it would in a *pseudo*-equatorial setting. This makes the effect of the C-3–O-3 bond less electron-withdrawing and allows for through-space electrostatic stabilization by the lone electron pairs on oxygen.

The stereoselectivity in glycosylations with furanosides that follow an S_N1 mechanism can be traced to the stereoselectivity inferred by the oxocarbenium ion. Woerpel and co-workers have established a model to account for the selectivity based on the E_3 and ^3E oxocarbenium ion conformations (Figure 2).[17–20] In this model, coined the two-conformer model, attack on the inside of the oxocarbenium ion is preferred over attack on the outside of the oxocarbenium ion. The basis of this rationale is the developing eclipsing interactions that occur in the transition state of the glycosylation reaction. When nucleophilic attack occurs on the outside of the oxocarbenium ion, the incoming nucleophile experiences eclipsing interactions with the *pseudo*-axially orientated substituent at C-2. The *pseudo*-equatorially orientated substituents at C-1 and C-2 also experience increased eclipsing interactions in the transition state upon rehybridization when a nucleophile attacks from the outside.

The stability of the oxocarbenium ion, dictated by its substituents, and the preference for inside attack leading to a more favorable transition state, leads to a model that can predict stereoselectivity based on oxocarbenium ion stability. The reasoning of this model is valid by the Hammond postulate: the geometry of the product-forming transition state is assumed to resemble the structure of the oxocarbenium ion intermediate, and the stereoselective preference of the ground-state oxocarbenium ion can therefore be taken as indicative of the reaction outcome (Figure 2). The ground state

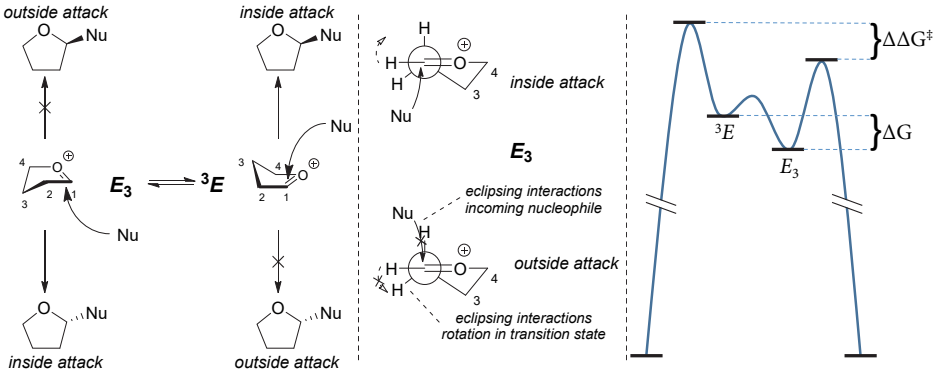

Figure 2. (left, middle) The two-conformer model, visualizing preferential nucleophilic attack from the inside face. Important rotations are denoted by dashed arrows. (right) Ground-state approximation to oxocarbenium ion stereoselectivity. $\Delta G \approx \Delta\Delta G^{\ddagger}$, energy levels are arbitrarily chosen for illustrative purposes. Reaction coordinate only visualized for the two inside attack pathways.

energy difference of two oxocarbenium ions (ΔG) is assumed to be similar to their transition state energy difference ($\Delta\Delta G^{\ddagger}$), thereby resulting in similar reaction rates of both inside attack pathways, and a product ratio mirroring the oxocarbenium ion ratio.

It can be difficult to predict which of the E_3-^3E envelopes is the more stable conformation on the basis of individual substituent effects, especially when there are conflicting orientational interests between the substituents. Furthermore, a change in protecting- or functional groups on the furanoside ring may have an unforeseen stereoelectronic influence, leading to less obvious geometries.[21,22] To assess the conformational behavior of furanosyl oxocarbenium ions, a method was devised based on Density Functional Theory (DFT), with which the relative stabilities of each conformation in the complete pseudo-rotational circle can be calculated, generating Conformational Energy Landscape (CEL) maps.[23] This method has been previously used by van Rijssel *et al.* to calculate the relative energies of furanosyl oxocarbenium ions of all four pentose furanosyl configurations (*arabino*-, *ribo*-, *lyxo*-, and *xylo*-configured, **49**, **53**, **57**, and **61**, Figure 3), bearing three *O*-methyl groups.[24,25] The results obtained by this method were in excellent agreement with experimental glycosylations (using the per-benzylated substrates, see also Table 1), and prompted further application of the DFT method to study relevant structural modifications. This chapter describes in detail the effects of the 2-fluoro, 2-azido, and 5-methyl uronate groups on the stability of the oxocarbenium ion conformations. The stereochemical outcome of experimental glycosylations is related to the structures of the intermediate oxocarbenium ions as revealed by the CEL maps.

Results and discussion

Glycosylations

Sixteen furanosides, comprising all four configurations of the D-pentofuranoses, with a 2-fluoro, 2-azido, or a 5-uronic acid ester substituent are studied, while the previously investigated fully benzylated donors are used for comparison.[24] The synthesis of all used furanosyl donors is described in Chapter 7.

The glycosyl donors of the C-2- and C-5-modified furanosides feature a trifluoro-*N*-phenylimidate anomeric leaving group (**9**-**20**, Table 1), since the corresponding acetyl donors proved inactive due to the presence of more electron-withdrawing substituents. Besides, allylations were preferred here over reactions with triethylsilane-*d* (TES-D) because the structure of the products could be determined with more ease, generally less side products were formed, the products could be easier separated from the contaminants, and the yields of the reactions were generally higher.[26] For the reactions of the C-2-azido donors TES-D was used because allyltrimethylsilane (allyl-TMS) did not lead to product formation even at higher temperatures (+5°C) and further increase of temperature led to degradation of the donor.

First the effect of these changes was probed by the condensation of tri-*O*-benzyl trifluoro-*N*-phenylimidate donors **5**-**8**, with allyl-TMS), showing nearly identical selectivities as those obtained previously by van Rijssel *et al*. with the four perbenzylated furanosyl acetates **1**-**4** with TES-D as the acceptor (see entries 1-4 *vs* entries 5-8, Table 1).[24] The high 1,2-*cis*-selectivity of all tri-*O*-benzyl furanosides (**1**-**8**, entries 1-8, Table 1) is apparent (α for *ribo*- and *xylo*-configured, β for *arabino*- and *lyxo*-configured substrates). The *ribo*- and *lyxo*-configured donors give solely the 1,2-*cis*-glycosylated products (**21**, **23**, **25**, **27**). The *xylo*-configured donors show poorer selectivity and a 85:15 α:β product ratio is obtained when both xylosyl donors are condensed with allyl-TMS (**28**) or TES-D (**24**). Arabinoside **1** is highly β-selective with TES-D (**21**) and forms a small amount of the other anomer when glycosylated as imidate **5** with allyl-TMS (**25**).

This 1,2-*cis*-selectivity largely remains in the series of C-2- and C-5-modified furanosides: all configurations except xylose are highly 1,2-*cis*-selective for all modifications tested. Rather strikingly, it thus appears that the nature of the substituents on furanosyl donors, have relatively little effect on the stereochemical outcome of the glycosylation reactions, when following a S_N1-like pathway. The 2-fluoroxyloside **36** is formed in a 70:30 α:β ratio, and the 2-azidoxyloside donor **20** gives a 85:15 mixture of

Table 1. Glycosylations of imidate donors **5-20**.[a]

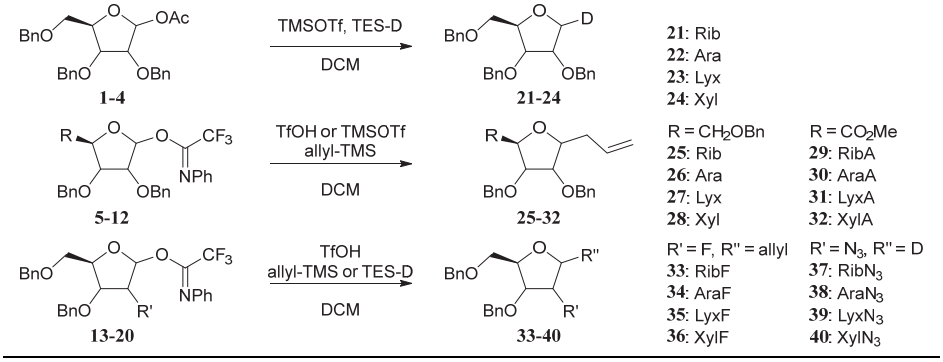

Entry	Donor	Donor configuration[b]	Acceptor	Temp. (°C)	Time (h)	Product	α : β	Yield (%)
1	**1**	β-Rib	2 eq. TES-D	-78	70	**21**	>98 : 2	50
2	**2**	α/β-Ara (2/1)	2 eq. TES-D	-78	165	**22**	<2 : 98	62
3	**3**	α-Lyx	2 eq. TES-D	-78	165	**23**	<2 : 98	100
4	**4**	α/β-Xyl (1/3)	2 eq. TES-D	-78	165	**24**	85 : 15	40
5	**5**	β-Rib	2 eq. allyl-TMS	-78	24	**25**	>98 : 2	[e]
6	**6**	α-Ara	2 eq. allyl-TMS	-78	24	**26**	10 : 90	[e]
7	**7**	α-Lyx	2 eq. allyl-TMS	-78	24	**27**	<2 : 98	[e]
8	**8**	α/β-Xyl (1/6)	2 eq. allyl-TMS	-78	24	**28**	85 : 15	[e]
9	**9**	β-RibA	4 eq. allyl-TMS	-20	100	**29**	>98 : 2	79
10	**10**	α/β-AraA (1/1)	4 eq. allyl-TMS	-20	100	**30**	5 : 95	76
11	**11**	α-LyxA[c]	4 eq. allyl-TMS	-20	100	**31**	<2 : 98	76
12	**12**	β-XylA	4 eq. allyl-TMS	-20	100	**32**	45 : 55	57[d]
13	**13**	β-RibF	4 eq. allyl-TMS	-20	100	**33**	>98 : 2	76
14	**14**	α-AraF[c]	4 eq. allyl-TMS	-20	100	**34**	<2 : 98	79
15	**15**	α-LyxF	4 eq. allyl-TMS	-20	100	**35**	<2 : 98	90
16	**16**	α/β-XylF (3/5)	4 eq. allyl-TMS	-20	100	**36**	70 : 30	62
17	**17**	β-RibN$_3$[c]	4 eq. TES-D	+5	100	**37**	>98 : 2	68
18	**18**	α-AraN$_3$[c]	4 eq. TES-D	+5	100	**38**	<2 : 98	57
19	**19**	β-LyxN$_3$[c]	4 eq. TES-D	+5	100	**39**	<2 : 98	59
20	**20**	α/β-XylN$_3$ (1/1)	4 eq. TES-D	+5	100	**40**	85 : 15	68[d]

Anomeric configuration established by HSQC-HECADE and NOESY NMR.[27–29] [a]Detailed experimental conditions are provided in the experimental section. [b]Imidates were assigned by ^{1}H NMR at +50°C in $CDCl_3$, but rotational dynamics still interfered with definite anomeric determination and the imidates are tentatively assigned based on ^{13}C chemical shift; imidate anomeric mixtures served as a reference. [c]These imidates were formed as an anomeric mixture and isolated as separate anomers, indicated is the anomer used in the reaction. [d]Calculated yields from isolated mixed fractions. [e]Yield not determined, ratios obtained from crude ^{1}H NMR.

anomers (product **40**), identical to the reaction of the corresponding tri-*O*-benzyl donor. The uronic acid xyloside donor **12** is the least selective (entry 12, Table 1), giving roughly equal amounts of both the α- and the β-product (**32**). The reactions of the xylosides also provided significant quantities of different side products. Beside **45**, the product originating from an intramolecular electrophilic aromatic substitution, the yet unreported trifluoro-*N*-phenylacetamide linked glycosides (**41**-**44**) were formed (Figure 4). The furanosides with other configurations only showed minor amounts of these side products.

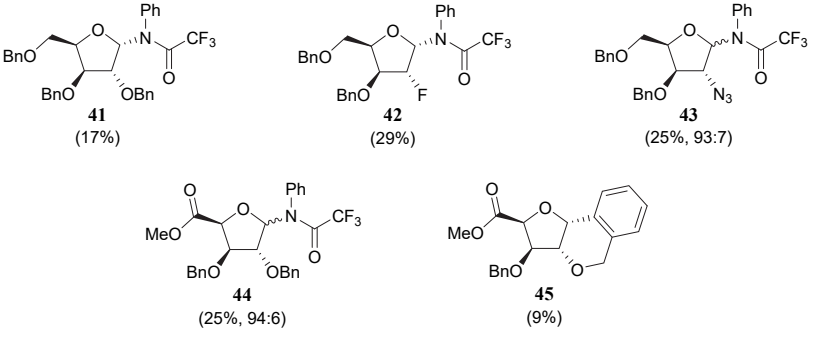

Figure 4. Side products **41**-**45** identified as side products, percentages obtained from the crude ^{1}H NMR.

Computations

With the experimental glycosylation stereoselectivity data available, the computational studies of the intermediate oxocarbenium ions were undertaken next. The oxocarbenium ions which are used in DFT calculations are displayed in Figure 3 and they are all protected with *O*-methyl ethers to limit rotational degrees of freedom and reduce computational cost.

The DFT calculations were executed by screening all the conformations on the pseudo-rotational circle, akin to the method described by van Rijssel *et al*. An initial geometry-optimized structure was taken as the base conformation and by changing the dihedral angles of the ring atoms, a set of 81 conformations was generated, with a maximum ring puckering of 40° (See Experimental section). While these dihedral angles were constrained, the other internal coordinates were allowed to change in the subsequent energy optimization calculations, performed by the Gaussian 03 software package,[30] at a computational level of B3LYP/6-311G**. Three separate sets of 81 conformations each were generated for the *gg*, *gt*, and *tg* C-4–C-5 rotamers respectively,

totaling 243 data points. For the uronic acids, two sets of 81 conformations, for the eclipsed and bisected structures, were assessed providing 162 data points. The energy obtained from the DFT calculations was corrected for solvation in DCM by a polarized continuum model (PCM). Additionaly, a Gibbs free energy correction was applied at the temperature of the glycosylation reactions.[31] The energy of all conformers was then visualized as a polar contour plot on the pseudo-rotational circle, with isoenergetic values as the contour lines, resulting in the Conformational Energy Landscape (CEL) maps (*vide infra*). Separate CEL maps are generated for the C-4–C-5 bond rotamers (*gg*, *gt*, *tg*, or eclipsed and bisected).

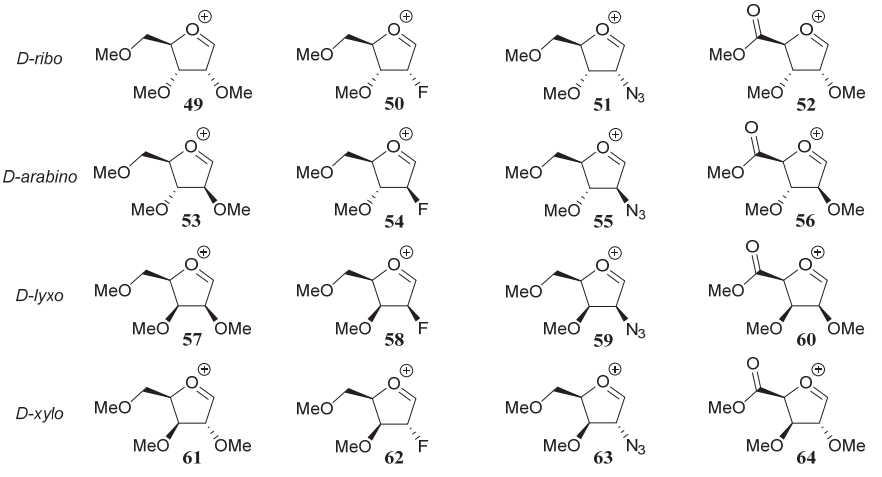

Figure 3. Oxocarbenium ions evaluated computationally in this chapter.

The modifications at C-2 and C-5 have been be examined for each configuration and Tables 2-5 report the CEL maps for each configuration, the contributions of each C-4–C-5 rotamer, the relative energy of the most favorable conformations, as well as the experimental stereoselectivities.

The results of the computational study of the *ribo*-configured furanosyl oxocarbenium ions **49-52** are provided in Table 2. The overall shape of the energy landscape is comparable for all four ions in the combined rotamer CEL maps, with the energy minima centered on the E_3 conformation, which places all the individual substituents in their most favorable orientation. The three individual rotamers provide similar maps for the different C-2 modifications, with *gg* being clearly the most favorable rotamer, as this species benefits from a stabilizing interaction of the O-5 lone pairs and the electron depleted anomeric center. The uronic acid has two low-energy C-4–C-5

Table 2. CEL maps of *ribo*-configured oxocarbenium ions **49**-**52**.

Ribose	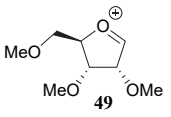 **49**	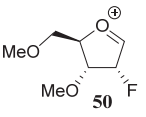 **50**	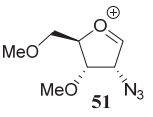 **51**	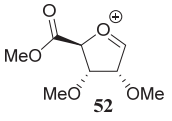 **52**
Combined rotamers	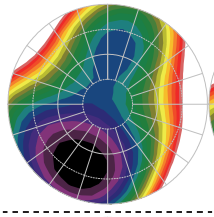	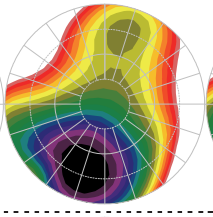	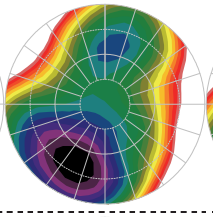	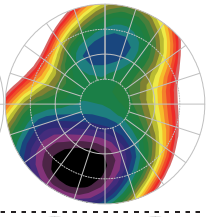
gg	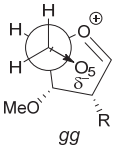 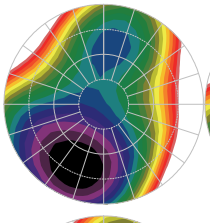	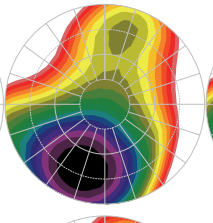	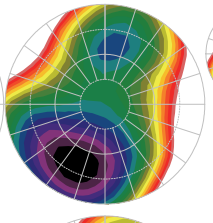	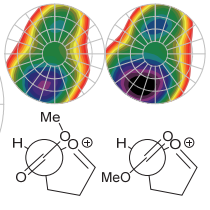
gt	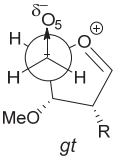 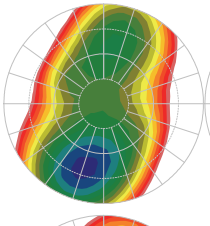	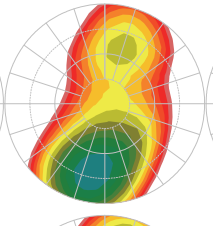	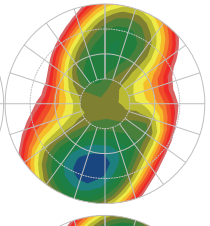	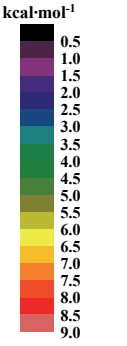
tg	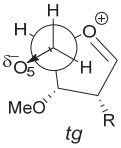 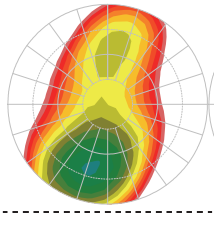	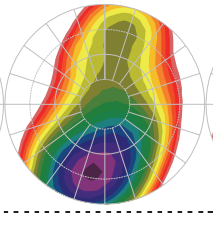	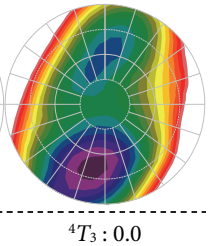	
Energies (kcal·mol^{-1})	E_3 : 0.0 $^4T_3$: 1.1 ^4E : 1.1 ^3E : 1.9	E_3 : 0.0 $^4T_3$: 0.5 ^4E : 1.5 ^3E : 5.2	$^4T_3$: 0.0 E_3 : 0.1 ^4E : 1.4 ^3E : 2.8	E_3 : 0.0 $^4T_3$: 0.3 ^3E : 2.5
	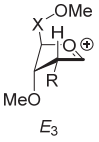 E_3	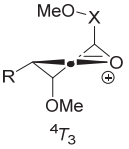 $^4T_3$	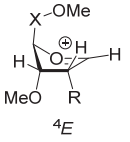 ^4E	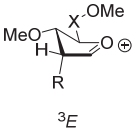 ^3E
Experimental (α : β)	>98 : 2	>98 : 2	>98 : 2	>98 : 2

R =OMe, F, or N_3; X = CH_2 or C=O.

rotamers, being the eclipsed and bisected ones. Apparently both can benefit from a charge-stabilizing interaction by the lone pairs of the oxygen atoms of the uronic acid ester. The CEL maps of both are similar, with the stabilization originating from the C=O being somewhat more favorable than the stabilization of the OMe group. The most appreciable structural difference that can be derived from the CEL maps of the four ribosyl oxocarbenium ions, is the stronger tendency of the fluorine atom to occupy a *pseudo*-equatorial orientation. The ^{3}E conformer of **50** is 5.2 kcal·mol^{-1} higher in energy than the lowest energy E_3 conformer, whereas this difference is only 1.9 kcal·mol^{-1} for **49** and around 2.5 kcal·mol^{-1} for **51** and **52**. The introduction of an electron-withdrawing substituent on C-2 or C-5 also led to the decrease of the relative energy of the twist $^{4}T_3$ structures, closely related to the E_3 conformation. Using the lowest energy E_3 conformers, or closely related $^{4}T_3$ structures, as product forming intermediates the formation of the 1,2-*cis*-products can be accounted for using the inside attack model. Thus the stereoelectronic effects of the C-2–OBn, C-2–F and C-2–N_3 on the stability and reactivity of the intermediate oxocarbenium ions appear to be very similar.

The CEL maps for *arabino*-configured furanosyl oxocarbenium ions **53-56** (depicted in Tabel 3) also have a very similar overall shape, with the energy minima at the ^{3}E conformations. The substituents for *arabino*-configured furanosyl oxocarbenium ions cannot simultaneously take up a most stabilizing orientation and the contribution of the C-2–H hyperconjugation seems to be most dominating, resulting in the ^{3}E as the lowest energy structure. The three C-4–C-5 rotamers show the expected order of stability: *gg* > *gt* > *tg*. There are small structural differences apparent caused by the stereoelectronic effects of the fluoro, and azido groups respectively. The ^{3}E conformation is clearly the most stable structure, but a second minimum appears on the other side of the CEL map at a minimally puckered E_3 conformation. The largest difference is seen for the C-2–N_3 *gg*-rotamer, where a second minimum-energy conformer can be found for structures adopting a $^{4}T_3/^{4}E$ conformation with minimal puckering, and one without any puckering (Figure 5). The uronic acid oxocarbenium ion **56** preferentially takes up a ^{3}E structure, with the related $^{3}T_4$ conformation being relatively close in energy (0.9 kcal·mol^{-1}).

The stereoselectivity of the condensation reactions of the arabinofuranosyl donors, which are all highly 1,2-*cis*-selective, may be explained using the $^{3}E/^{3}T_4$ structures as product forming intermediates. This would indicate that attack on the more flat C-2–N_3 oxocarbenium ions is relatively unfavorable.

Table 3. CEL maps of *arabino*-configured oxocarbenium ions **53-56**.

Arabinose	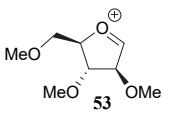 **53**	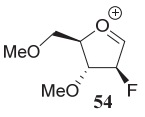 **54**	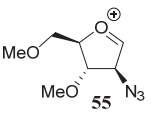 **55**	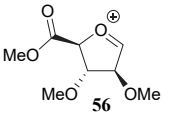 **56**
Combined rotamers	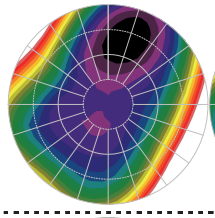	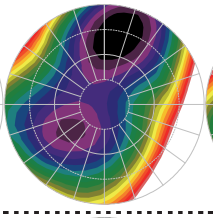	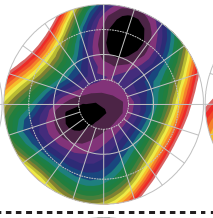	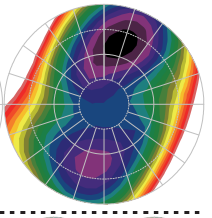
gg	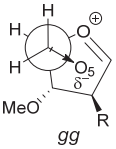 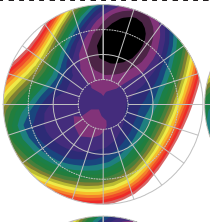	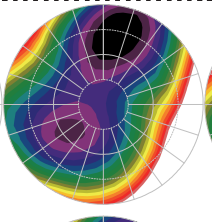	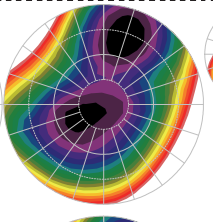	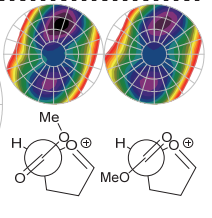
gt	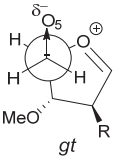 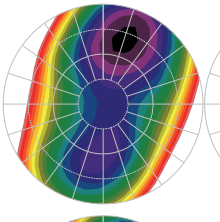	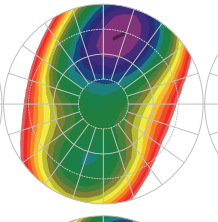	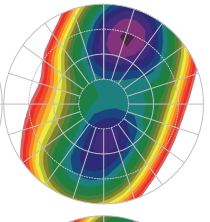	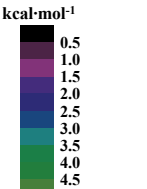
tg	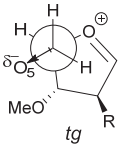 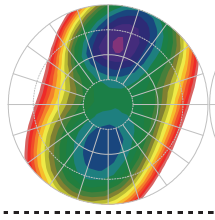	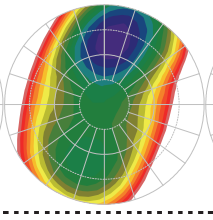	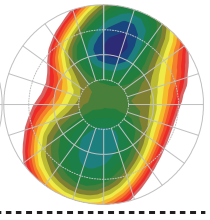	
Energies (kcal·mol^{-1})	^3E : 0.0 *flat*-E_3 : 1.2 E_3 : 2.2	^3E : 0.0 *flat*-^4E : 0.6 *flat*-$^4T_3$: 1.1 *flat*-E_3 : 1.2	^3E : 0.0 *flat*-^4E : 0.3 *flat*: 0.4 *flat*-E_3 : 0.9	^3E : 0.0 $^3T_4$: 0.9 E_3 : 1.2
	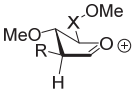 ^3E	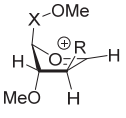 ^4E	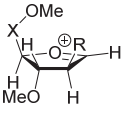 *flat*	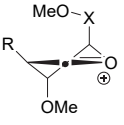 $^4T_3$	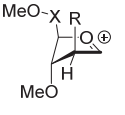 E_3	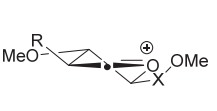 $^3T_4$
Experimental (α : β)	<2 : 98	<2 : 98	<2 : 98	5 : 95

R =OMe, F, or N_3; X = CH_2 or C=O.

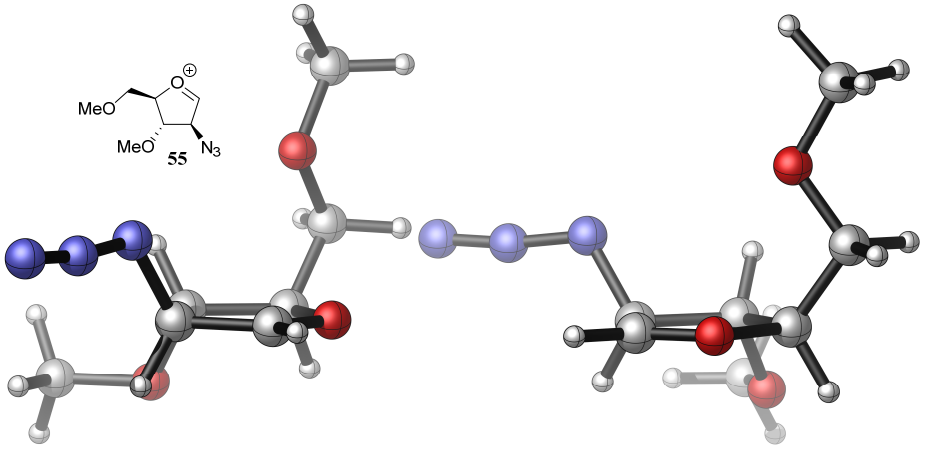

Figure 5. Ball-stick model of the *flat* conformation of 2-azidoarabinosyl oxocarbenium ion **55**, viewed through the C-2–C-3 bond and C-1–C-2 bond respectively.

All *lyxo*-configured oxocarbenium ions **57**-**60** (Table 4) show a single energy minimum on the ^{3}E side of the CEL map. The difference in energy between this structure and the other conformers appears to be even larger than the energy differences observed for the ribosyl oxocarbenium ions. This can be understood by realizing that the 'inverted' envelope, the E_3, not only loses the stabilizing interactions of the C-2 and C-3 substituents, but also experiences severe 1,3-diaxial interactions between the C-2 and C-4 groups, especially for the electronically most favorable *gg*-rotamer. In the most stable ^{3}E conformer, the steric interaction between the C-5–OMe and the C-3–OMe (a 1,3-diaxial like interaction) increases the relative energy of the *gg*-rotamer, and the *gt*-rotamer is the most favorable rotamer providing the energy minimum in the overall CEL map. Also in the *lyxo*-case, the effect of the different substituents is minimal, although structures occupying a $^{3}T_{4}$ conformation are relatively favorable for all three modifications (being 1.2-2.1 kcal·mol^{-1} higher in energy than the neighboring E_3 envelopes). Again the lowest energy oxocarbenium ions account for the observed experimental all-*cis* stereoselectivity, following the inside attack model.

Table 4. CEL maps of *lyxo*-configured oxocarbenium ions **57-60**.

Lyxose	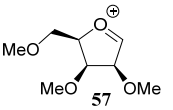 **57**	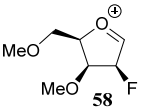 **58**	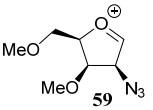 **59**	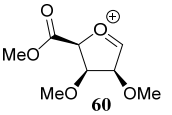 **60**
Combined rotamers	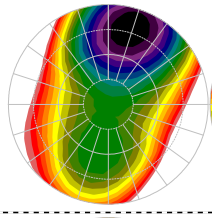	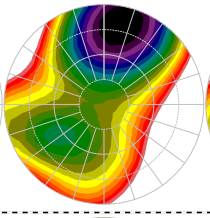	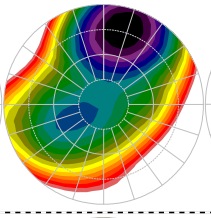	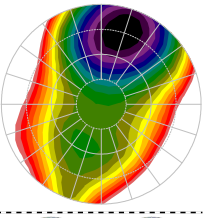
gg	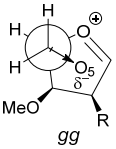 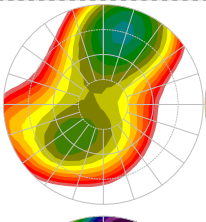	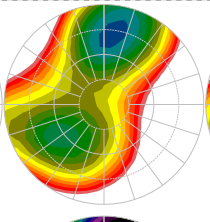	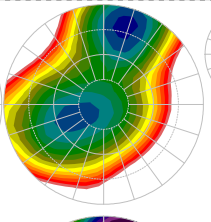	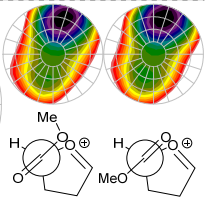
gt	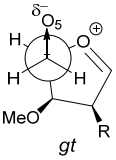 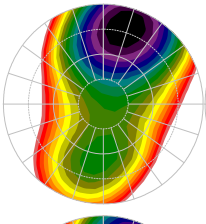	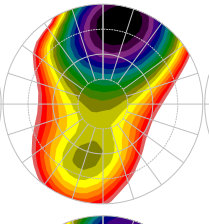	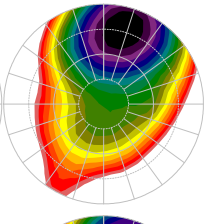	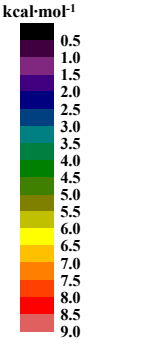
tg	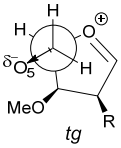 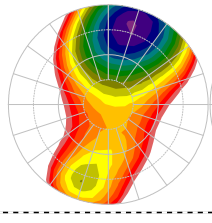	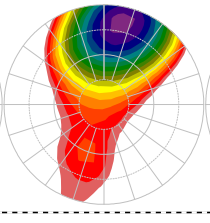	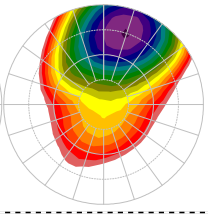	
Energies (kcal·mol^{-1})	^3E : 0.0 E_3 : 4.2	^3E : 0.0 *flat*-$^3T_4$: 2.1 E_3 : 4.7	^3E : 0.0 $^3T_4$: 1.4 *flat*-E_3 : 3.2	^3E : 0.0 $^3T_4$: 1.2 E_3 : 4.4
	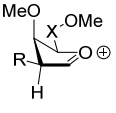 ^3E	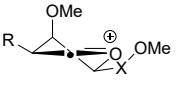 $^3T_4$	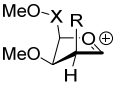 E_3	
Experimental (α : β)	<2 : 98	<2 : 98	<2 : 98	<2 : 98

R =OMe, F, or N_3; X = CH_2 or C=O.

Finally, the *xylo*-configured oxocarbenium ions **61**-**64** (Table 5) were assessed. Again, the CEL maps of the differently functionalized xylosides appear to be rather similar. Two minima are apparent on either side of the CEL maps. These minima originate from C-4–C-5 rotamers, with the *gg*- and *gt*-rotamers leading to low energy E_3-like and ^3E-like structures respectively. The energy minima located on the south side of the CEL maps are relatively 'broad' and not only encompass the E_3 conformations but also, as noted earlier by van Rijssel *et al.*, the $^4T_3$ structures, and perhaps more striking, the ^4E envelope conformation. This latter conformer is in fact the lowest energy species for 2-fluoroxyloside **62** and xylosyl uronate **64**. This conformation is unable to use the stabilizing effect of the O-3 lone electron pairs, or the hyperconjugation of the C–H bond on C-2 to its full extent (Figure 6). Instead, the driving stabilization now appears to be the interaction of the C-5–*O*-benzyl with the anomeric center. In the ^4E conformation, the steric interactions between C-5 and the substituents at C-3 and the C-2–H are reduced when compared to the sterically unfavorable situation in the E_3 conformer.

When the relative energy of the different configurations is compared, it becomes clear that the xylose oxocarbenium ions are higher in energy than their configurational counterparts. This may, in part, account for the higher amount of side products formed in the reactions of the xylosyl donors.[32] The established broad energy minima may be at the basis for the poor stereoselectivity observed in the condensations of the xylosyl donors as attack of the ^4E conformers (See Figure 6) may occur from both sides of the ring.

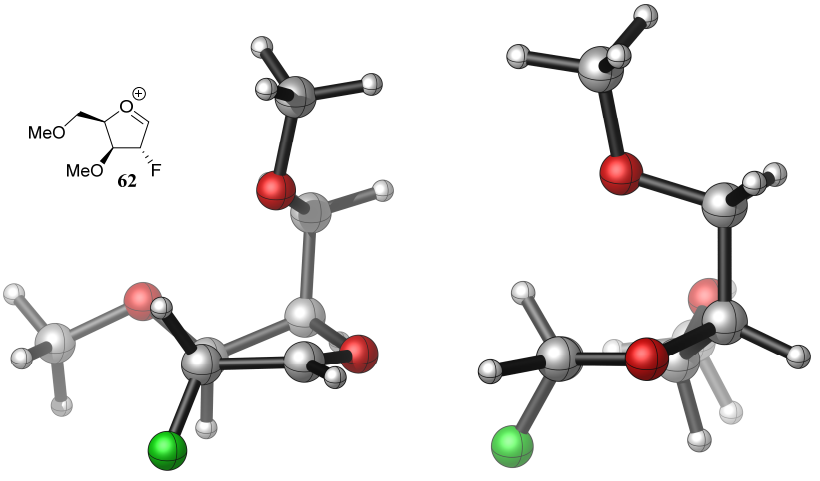

Figure 6. Ball-stick model of the ^4E conformation of 2-fluoroxylosyl oxocarbenium ion **62**, viewed through the C-2–C-3 bond and C-1–C-2 bond respectively.

Table 5. CEL maps of *xylo*-configured oxocarbenium ions **61-64**.

Xylose	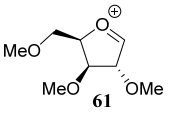 **61**	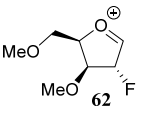 **62**	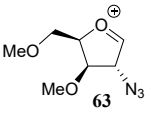 **63**	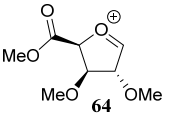 **64**
Combined rotamers	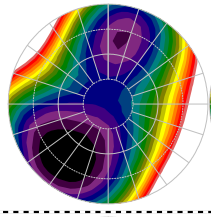	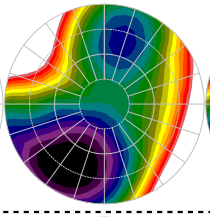	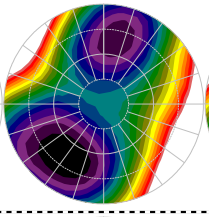	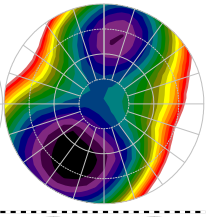
gg	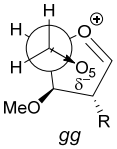 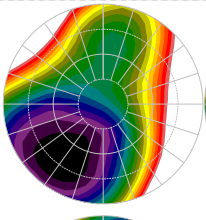	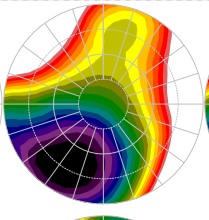	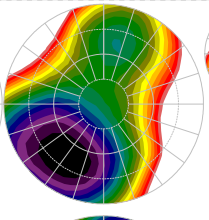	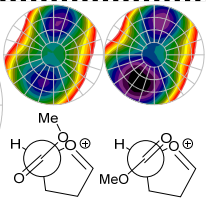
gt	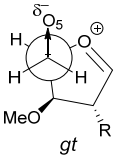 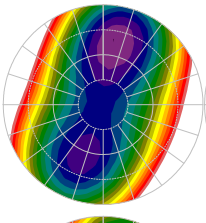	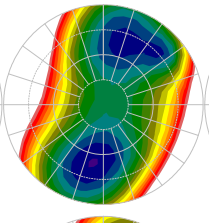	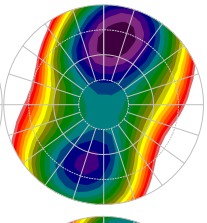	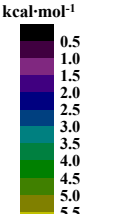
tg	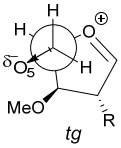 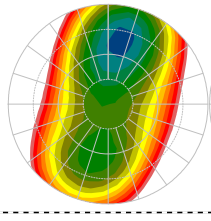	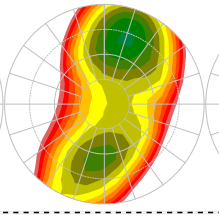	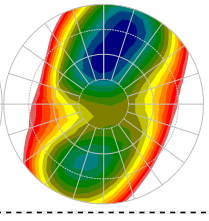	
Energies (kcal·mol^{-1})	$^4T_3$: 0.0 ^4E : 0.4 E_3 : 0.4 ^3E : 1.0	$^4T_3$: 0.0 ^4E : 0.0 E_3 : 0.1 ^3E : 2.3	$^4T_3$: 0.0 E_3 : 0.2 ^4E : 0.5 ^3E : 0.8	^4E : 0.0 E_3 : 0.2 *flattened*-$^4T_3$: 0.4 ^3E : 1.1
	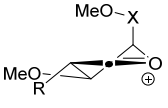 $^4T_3$	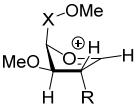 ^4E	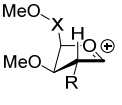 E_3	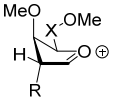 ^3E
Experimental (α : β)	85 : 15	70 : 30	85 : 15	45 : 55

R =OMe, F, or N_3; X = CH_2 or C=O.

Conclusions

A set of twelve functionalized furanosides has been glycosylated under conditions favoring an S_N1-type substitution reaction with allyltrimethylsilane or triethylsilane-*d* to investigate the stereoselectivity of these reactions. The experimental results have been complemented by computational studies, generating Conformational Energy Landscape (CEL) maps for the intermediate oxocarbenium ions. Striking similarities have been observed for the CEL maps of the oxocarbenium ions featuring different C-2 and C-5 substituents and –as a result– very similar stereoselectivities are obtained in the glycosylations of the different donors. Nonetheless, the CEL map method also revealed conformers different from the ^3E-E_3 pair as relatively stable conformers and structural deviations to ^4E, $^4T_3$, $^3T_4$ and flat conformations have been revealed in some cases for the 2-fluoro, 2-azido, and 5-methyl uronate substituted species. The changes in the population of the different conformational states of the reactive intermediate only had a minor effect on the outcome of the glycosylations, which where across the board highly 1,2-*cis*-selective, except for the *xylo*-configured furanosides which consistently provided anomeric mixtures. The appearance of more low-energy conformations for the *xylo*-configured oxocarbenium ions could account for the erosion of stereoselectivity. CEL maps with a localized single energy minimum corresponded to reactions that are completely stereoselective. Overall, the study described here has shown that the nature of the substituent, C-2–OBn *vs* –F or $-N_3$ and C-4–CH_2OBn *vs* $-CO_2$Me, does not significantly affect the structure of the intermediate ions and the course of the S_N1-type reactions studied here. This stands in sharp contrast to the effect that these substituents have in glycosylations of pyranosyl donors (See for example chapter 4 and 6). The effect of the different substituents in this case can probably best be reconciled with a change in the S_N2-S_N1 reaction mechanism continuum.

Experimental section

General procedure for furanoside imidate glycosylations. The imidate donor (0.1 mmol, 1 eq.) was coevaporated twice with dry toluene and then dissolved in dry DCM (1 mL). Activated 3 Å molecular sieves and the acceptor (2 or 4 eq.) were added and the solution was stirred for 30 min at room temperature under an inert atmosphere (N_2 or Ar). The reaction mixture was cooled to the indicated temperature and a freshly prepared stock solution (0.2 M in DCM) of TMSOTf or TfOH was introduced via syringe (50 µL, 0.01 mmol, 0.1 eq.). The reaction mixture was stirred for 1-4 days at the indicated temperature, and was then quenched by the addition of sat. aq. $NaHCO_3$. The mixture was diluted with H_2O and twice extracted with DCM. The combined organic layers were dried with $MgSO_4$, filtered, and concentrated *in vacuo*. The residue was purified by flash column chromatography (1/0 to 80/20 pentane/Et_2O) to provide the glycosylated furanoside.

General procedure for quantum mechanical calculations. Analogous to the work of van Rijssel,[24] all calculations were performed with DFT calculations with the B3LYP hybrid functional. The starting conformer for the Conformational Energy Landscapes (CEL) was obtained by a conformer distribution search in the Spartan 10 program in the gas phase, with a 6-31G(d) basis set. All resulting geometries were further optimized at the 6-311G(d,p) level in the Gaussian 03 program, with a polarized continuum model (PCM) to correct for solvation in dichloromethane, and further corrected for their zero-point energy (ZPE). The geometry with the lowest, ZPE corrected solvated energy, was selected and used as the starting geometry for the CEL. Two dihedral angles of the five-membered ring were constrained: C4-O4-C1-C2 and C1-C2-C3-C4 by scanning with 10° per step, over 9 steps (-40° to 40°), totaling 81 conformations spanning the entire pseudo rotational sphere with a maximum puckering amplitude (τ_m) of 40°. All other internal coordinates were unconstrained. Three separate staggered rotamers (*gg*, *gt*, *tg*) of the O4-C4-C5-O5 dihedral angle (-65°, 65°, 175°) were considered and their CEL maps were calculated separately by pre-rotating the C4-C5 bond (not constrained), bringing the total conformations for each configuration to 243 geometries. The final denoted free Gibbs energy was calculated using Equation (1) in which ΔE_{gas} is the gas-phase energy (electronic energy), ΔG^T_{gas} (T = 298.15 K and pressure = 1 atm.) is the sum of corrections from the electronic energy to free Gibbs energy in the harmonic oscillator approximation also including zero-point-vibrational energy, and ΔG^T_{solv} is their corresponding free solvation Gibbs energy.

$$\Delta G^T_{in\ solution} = \Delta E_{gas} + \Delta G^T_{gas} + \Delta G_{solv} \quad (1)$$

$$= \Delta G^T_{gas} + \Delta G_{solv}$$

All found minima were checked for negative frequencies. The CEL was visualized as a polar contour plot by the Origin pro 9 software, with the energy plotted as 0.5 kcal·mol^{-1} colored intervals, the phase angle P as the azimuth angle and the puckering amplitude (τ_m) as the radius, with a smoothing factor of 0.001. The computed stereoselectivity was based on the ^3E - E_3 two conformer (inside-attack) model, as the ratio of conformers obtained from the Boltzmann distribution over these two conformers, at the temperature of the experiment.

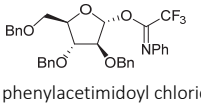

2,3,5-tri-*O*-benzyl-1-*O*-(*N*-[phenyl]trifluoroacetimidoyl)-α-D-arabinofuranoside (6). The arabinofuranose lactol[24] (421 mg, 1 mmol) was dissolved in acetone (6 mL) and H_2O (0.1 mL) and cooled to 0°C. Cs_2CO_3 (358 mg, 1,1 mmol, 1.1 eq.) and 2,2,2-trifluoro-*N*-phenylacetimidoyl chloride (317 µL, 2 mmol, 2 eq.) were added and the reaction mixture stirred overnight. Very little conversion was observed (TLC-analysis), therefore DBU (0.12 mL) was added and the conversion was complete immediately. The reaction mixture was reduced in volume under reduced pressure and H_2O was added. The aqueous phase was extracted twice with DCM and the combined organic layers were dried with Na_2SO_4, filtered, and concentrated under reduced pressure. Flash column chromatography (0-15% Et_2O/pentane, with 0.5% Et_3N) of the residue provided the target imidate donor. Yield = 425 mg, 0.72 mmol, 72% as a waxy solid. R_f: 0.81 (85/15 pentane/Et_2O). ^{1}H NMR ($CDCl_3$, *T* = 323 K, 400 MHz, HH-COSY, HSQC): δ 7.32 – 7.22 (m, 17H, CH_{arom}), 7.09 – 7.01 (m, 1H, NPh), 6.80 (d, 2H, *J* = 8.0 Hz, NPh), 6.27 (bs, 1H, H-1), 4.60 – 4.47 (m, 6H, 3xCH_2 Bn), 4.45 (q, 1H, *J* = 5.1 Hz, H-4), 4.23 (d, 1H, *J* = 1.8 Hz, H-2), 4.03 (dd, 1H, *J* = 5.5, 2.0 Hz, H-3), 3.63 (d, 2H, *J* = 5.1 Hz, H-5, H-5); ^{13}C-APT NMR ($CDCl_3$, *T* = 323 K, 101 MHz, HSQC): δ 144.0 (C_q NPh), 138.1, 137.9, 137.4 (C_q Bn), 128.8, 128.5, 128.5, 128.4, 127.9, 127.9, 127.8, 127.7, 124.3, 119.8 (CH_{arom}), 104.0 (C-1), 87.0 (C-2), 84.1 (C-4), 83.8 (C-3), 73.5, 72.3 (CH_2 Bn), 69.7 (C-5); HRMS: $[M+Na]^+$ calcd for $C_{34}H_{32}F_3NO_5Na$ 614.21217, found 614.21248.

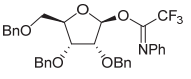

2,3,5-tri-*O*-benzyl-1-*O*-(*N*-[phenyl]trifluoroacetimidoyl)-β-D-ribofuranoside (5). The ribofuranose lactol[24] (421 mg, 1 mmol) was dissolved in acetone (6 mL) and H_2O (0.1 mL) and cooled to 0°C. Cs_2CO_3 (489 mg, 1,5 mmol, 1.5 eq.) and 2,2,2-trifluoro-*N*-phenylacetimidoyl chloride (238 µL, 1.5 mmol, 1.5 eq.) were added and the reaction mixture stirred for 2 days. The reaction mixture was reduced in volume under reduced pressure and H_2O was added. The aqueous phase was extracted twice with DCM and the combined organic layers were dried with Na_2SO_4, filtered, and concentrated under reduced pressure. Flash column chromatography (0-15% Et_2O/pentane, with 0.5% Et_3N) of the residue provided the target imidate donor. Yield = 327 mg, 0.55 mmol, 55% as a colourless oil. R_f: 0.15 (95/5 pentane/Et_2O). Spectroscopic data were in accord with those previously reported.[33] ^{1}H NMR ($CDCl_3$, *T* = 295 K, 400 MHz, HH-COSY, HSQC): δ 7.34 – 7.26 (m, 17H, CH_{arom}), 7.14 – 7.06 (m, 1H, NPh), 6.80 (d, 2H, *J* = 7.5 Hz, NPh), 6.33 (bs, 1H, H-1), 4.75 – 4.50 (m, 5H, 2xCH_2 Bn, C*H*H Bn), 4.49 – 4.43 (m, 2H, CH*H* Bn, H-4), 4.16 (dd, 1H, *J* = 7.3, 4.7 Hz, H-3), 4.07 (d, 1H, *J* = 4.0 Hz, H-2), 3.71 (dd, 1H, *J* = 11.0, 3.1 Hz, H-5), 3.59 (dd, 1H, *J* = 11.0, 4.9 Hz, H-5); ^{13}C-APT NMR ($CDCl_3$, *T* = 295 K, 101 MHz, HSQC): δ 143.8 (C_q NPh), 138.2, 137.5, 137.4 (C_q Bn), 128.8, 128.5, 128.5, 128.4, 128.2, 128.1, 128.0, 127.9, 127.6, 124.3, 119.7 (CH_{arom}), 102.5 (C-1), 82.2 (C-4), 78.5 (C-2), 77.3 (C-3), 73.3, 72.7, 72.3 (CH_2 Bn), 70.0 (C-5).

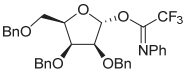

2,3,5-tri-*O*-benzyl-1-*O*-(*N*-[phenyl]trifluoroacetimidoyl)-α-D-lyxofuranoside (7). The lyxofuranose lactol[24] (660 mg, 1,58 mmol) was dissolved in acetone (8 mL) and H_2O (0.5 mL) and cooled to 0°C. Cs_2CO_3 (619 mg, 1,9 mmol, 1.2 eq.) and 2,2,2-trifluoro-*N*-phenylacetimidoyl chloride (500 µL, 3.17 mmol, 2 eq.) were added and the reaction mixture stirred overnight. Very little conversion was observed (TLC-analysis), therefore DBU (0.2 mL) was added and the conversion was complete immediately. The reaction mixture was reduced in volume under reduced pressure and coevaporated with dioxane and toluene. The residue was dissolved in DCM and filtered over Celite, the filtrate was concentrated under reduced pressure. Flash column chromatography (0-15% Et_2O/pentane, with 0.5% Et_3N) of the residue provided the target imidate donor. Yield = 930 mg, 1.57 mmol, 100% as a white solid. R_f: 0.8 (85/15 pentane/Et_2O). ^{1}H NMR ($CDCl_3$, *T* = 323 K, 400 MHz, HH-COSY, HSQC): δ 7.34 – 7.20 (m, 17H, CH_{arom}), 7.09 – 7.01 (m, 1H, NPh), 6.78 (d, 2H, *J* = 8.0 Hz, NPh), 6.31 (bs, 1H, H-1), 4.68 – 4.44 (m, 7H, 3xCH_2 Bn, H-4), 4.25 (t, 1H, *J* = 5.1 Hz, H-3), 4.13 (d, 1H, *J* = 4.2 Hz, H-2), 3.83 (dd, 1H, *J* = 10.5, 4.7 Hz, H-5), 3.76 (dd, 1H, *J* = 10.4, 7.3 Hz, H-5); ^{13}C-APT NMR ($CDCl_3$, *T* = 323 K, 101 MHz, HSQC): δ 143.9 (C_q NPh), 138.2, 137.9, 137.5 (C_q Bn), 129.3, 128.8, 128.5, 128.4, 128.4, 128.0, 127.9, 127.8, 127.7, 124.4, 119.7 (CH_{arom}), 103.0 (C-1), 81.7 (C-2), 80.5 (C-4), 77.4 (C-3), 73.5, 73.5, 72.9 (CH_2 Bn), 69.5 (C-5).

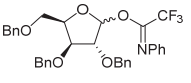

2,3,5-tri-*O*-benzyl-1-*O*-(*N*-[phenyl]trifluoroacetimidoyl)-α/β-D-xylofuranoside (8). The xylofuranose lactol[24] (421 mg, 1 mmol) was dissolved in acetone (10 mL) and cooled to 0°C. 2,2,2-Trifluoro-*N*-phenylacetimidoyl chloride (190 µL, 1.2 mmol, 1.2 eq.) and DBU (165 µL, 1.1 mmol, 1.1 eq.) were added and the reaction mixture stirred for 1 h. The reaction mixture was reduced in volume under reduced pressure and H_2O was added. The aqueous phase was extracted twice with DCM and the combined organic layers were dried with Na_2SO_4, filtered, and concentrated under reduced pressure. Flash column chromatography (0-15% Et_2O/pentane, with 0.5% Et_3N) of the residue provided the target imidate donor. Yield = 427 mg, 0.72 mmol, 72% as a waxy solid. R_f: 0.38 and 0.47 (9/1 pentane/Et_2O). Data for the β-anomer: ^{1}H NMR ($CDCl_3$, *T* = 295 K, 400 MHz, HH-COSY, HSQC): δ 7.34 – 7.18 (m, 17H, CH_{arom}), 7.05 (t, 1H, *J* = 7.4 Hz, NPh), 6.77 (d, 2H, *J* = 7.6 Hz, NPh), 6.30 (bs, 1H, H-1), 4.65 (q, 1H, *J* = 5.6 Hz, H-4), 4.60 – 4.42 (m, 6H, 3xCH_2 Bn), 4.24 (s, 1H, H-2), 4.10 (d, 1H, *J* = 5.4 Hz, H-3), 3.86 (dd, 1H, *J* = 10.4, 5.1 Hz, H-5), 3.80 (dd, 1H, *J* = 10.2, 7.2 Hz, H-5); ^{13}C-APT NMR ($CDCl_3$, *T* = 295 K, 101 MHz, HSQC): δ 143.9 (C_q NPh), 138.2, 137.7, 137.2 (C_q Bn), 129.1, 128.7, 128.5, 128.4, 128.3, 128.0, 127.8, 127.7, 127.6, 127.5, 124.2, 119.6 (CH_{arom}), 103.5 (C-1), 84.5 (C-2), 83.0 (C-4), 81.1 (C-3), 73.4, 72.4, 72.1 (CH_2 Bn), 69.1 (C-5).

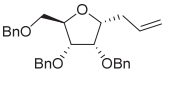

Allyl 2,3,5-tri-*O*-benzyl-1-deoxy-α-D-ribofuranoside (25). Donor **5** and allyltrimethylsilane (2 eq.) were condensed using the general procedure for furanosyl imidate glycosylations at -78°C for 24 h with TMSOTf as the promotor. R_f: 0.27 (19/1 pentane/EtOAc). Spectroscopic data were in accord with those previously reported.[34] ^{1}H NMR ($CDCl_3$, 400 MHz, HH-COSY, HSQC): δ 7.40 – 7.23 (m, 15H, CH_{arom}), 5.79 (ddt, 1H, *J* = 17.1, 10.2, 6.9 Hz, CH allyl), 5.10 (dq, 1H, *J* = 17.2, 1.5 Hz, C*H*H allyl), 5.04 (ddt, 1H, *J* = 10.2, 2.1, 1.1 Hz, CH*H* allyl), 4.81 (d, 1H, *J* = 11.7 Hz, C*H*H Bn), 4.64 – 4.45 (m, 5H, CH*H* Bn, 2xCH_2 Bn), 4.21 (dt, 1H, *J* = 7.1, 3.5 Hz, H-4), 4.10 (dd, 1H, *J* = 7.1, 4.3 Hz, H-3), 4.05 (td, 1H, *J* = 7.0, 3.9 Hz, H-1), 3.98 (t, 1H, *J* = 4.1 Hz, H-2), 3.63 (dd, 1H, *J* = 10.7, 3.3 Hz, H-5), 3.52 (dd, 1H, *J* = 10.7, 3.8 Hz, H-5), 2.51 (t, 2H, *J* = 7.0 Hz, CH_2 allylic); ^{13}C-APT NMR ($CDCl_3$, 101 MHz, HSQC): δ 138.6, 138.4, 138.1 (C_q Bn), 135.1 (CH allyl), 128.5, 128.4, 128.4, 127.9, 127.8, 127.8, 127.7, 127.7 (CH_{arom}), 117.0 (CH_2 allyl), 80.2 (C-1), 80.1 (C-3), 79.6 (C-4), 77.7 (C-2), 73.5, 73.4, 72.8 (CH_2 Bn), 70.2 (C-5), 34.4 (CH_2 allylic); HRMS: $[M+NH_4]^+$ calcd for $C_{29}H_{36}NO_4$ 462.26389, found 462.26382.

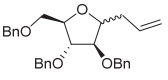

Allyl 2,3,5-tri-*O*-benzyl-1-deoxy-α/β-D-arabinofuranoside (26). Donor **6** and allyltrimethylsilane (2 eq.) were condensed using the general procedure for furanosyl imidate glycosylations at -78°C for 24 h with TMSOTf as the promotor. (α:β = 10:90). Spectroscopic data were in accord with those previously reported.[35] ^{1}H NMR ($CDCl_3$, 400 MHz, HH-COSY, HSQC): δ 7.36 – 7.23 (m, 15H, CH_{arom}), 5.80 (ddt, 1H, *J* = 17.1, 10.2, 7.0 Hz, CH allyl), 5.15 – 5.00 (m, 2H, CH_2 allyl), 4.61 – 4.47 (m, 5H, 2x CH_2 Bn, C*H*H Bn), 4.36 (d, 1H, *J* = 11.9 Hz, CH*H* Bn), 4.08 (td, 1H, *J* = 6.7, 2.8 Hz, H-4), 4.03 (td, 1H, *J* = 7.0, 3.5 Hz, H-1), 3.92 (d, 1H, *J* = 2.7 Hz, H-3), 3.81 (d, 1H, *J* = 3.5 Hz, H-2), 3.63 (dd, 1H, *J* = 9.8, 5.8 Hz, H-5), 3.51 (dd, 1H, *J* = 9.8, 6.9 Hz, H-5), 2.52 – 2.47 (m, 2H, CH_2 allylic); ^{13}C-APT NMR ($CDCl_3$, 101 MHz, HSQC): δ 138.3, 138.0, 137.9 (C_q Bn), 135.0 (CH allyl), 128.6, 128.5, 128.4, 127.9, 127.8, 127.8, 127.8, 127.7 (CH_{arom}), 117.1 (CH_2 allyl), 83.8 (C-3), 82.9 (C-2), 82.8 (C-4), 81.1 (C-1), 73.4, 71.5, 71.4 (CH_2 Bn), 70.7 (C-5), 33.3 (CH_2 allylic).

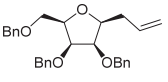

Allyl 2,3,5-tri-*O*-benzyl-1-deoxy-β-D-lyxofuranoside (27). Donor **7** and allyltrimethylsilane (2 eq.) were condensed using the general procedure for furanosyl imidate glycosylations at -78°C for 24 h with TMSOTf as the promotor. R_f: 0.47 (9/1 pentane/EtOAc). ^{1}H NMR ($CDCl_3$, 400 MHz, HH-COSY, HSQC): δ 7.36 – 7.24 (m, 15H, CH_{arom}), 5.82 (ddt, 1H, *J* = 17.1, 10.2, 7.0 Hz, CH allyl), 5.07 (dq, 1H, *J* = 17.1, 1.5 Hz, C*H*H allyl), 5.02 (ddt, 1H, *J* = 10.2, 2.2, 1.2 Hz, CH*H* allyl), 4.76 (d, 1H, *J* = 11.8 Hz, C*H*H Bn), 4.68 (d, 1H, *J* = 11.9 Hz, C*H*H Bn), 4.61 (d, 1H, *J* = 11.9 Hz, CH*H* Bn), 4.59 (d, 1H, *J* = 12.1 Hz, C*H*H Bn), 4.54 (d, 1H, *J* = 11.8 Hz, CH*H* Bn), 4.52 (d, 1H, *J* = 12.1 Hz, CH*H* Bn), 4.24 – 4.19 (m, 1H, H-4), 4.17 (dd, 1H, *J* = 6.1, 3.9 Hz, H-3), 4.01 – 3.94 (m, 2H, H-1, H-2), 3.83 (dd, 1H, *J* = 10.1, 4.8 Hz, H-5), 3.72 (dd, 1H, *J* = 10.1, 6.6 Hz, H-5), 2.53 – 2.46 (m, 2H, CH_2 allylic); ^{13}C-APT NMR ($CDCl_3$, 101 MHz, HSQC): δ 138.6, 138.5, 138.4 (C_q Bn), 135.6 (CH allyl), 128.5, 128.4, 128.4, 127.9, 127.7, 127.7, 127.6, 127.5 (CH_{arom}), 116.7 (CH_2 allyl), 79.6 (C-3), 79.1 (C-1), 78.9 (C-2), 78.0 (C-4), 73.4, 73.3, 73.3 (CH_2 Bn), 70.5 (C-5), 35.4 (CH allylic); ^{13}C HSQC-HECADE NMR ($CDCl_3$, 101 MHz): $^2J_{C1,H2}$ = +1.0 Hz, $^2J_{C2,H1}$ = +1.5 Hz, $^3J_{H2,C\text{-}allyl}$ = +1.6 Hz; HRMS: $[M+H]^+$ calcd for $C_{29}H_{33}O_4$ 445.23709, found 445.23704.

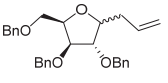

Allyl 2,3,5-tri-*O*-benzyl-1-deoxy-α/β-D-xylofuranoside (28). Donor **8** and allyltrimethylsilane (2 eq.) were condensed using the general procedure for furanosyl imidate glycosylations at -78°C for 24 h with TMSOTf as the promotor. R_f: 0.38 (92/8 pentane/Et_2O). Spectroscopic data were in accord with those previously reported for the β-anomer.[36] Data for the α-anomer: ^{1}H NMR ($CDCl_3$, 400 MHz, HH-COSY, HSQC): δ 7.40 – 7.22 (m, 15H, CH_{arom}), 5.78 (ddt, 1H, *J* = 17.1, 10.2, 6.9 Hz, CH allyl), 5.10 (dq, 1H, *J* = 17.2, 1.6 Hz, C*H*H allyl), 5.02 (ddd, 1H, *J* = 10.2, 2.2, 1.1 Hz, CH*H* allyl), 4.64 – 4.35 (m, 6H, 3xCH_2 Bn), 4.37 (td, 1H, *J* = 6.3, 4.1 Hz, H-4), 4.16 (td, 1H, *J* = 7.1, 3.7 Hz, H-1), 4.03 (dd, 1H, *J* = 4.1, 1.1 Hz, H-3), 3.83 (dd, 1H, *J* = 3.7, 1.1 Hz, H-2), 3.72 (dd, 1H, *J* = 9.6, 6.4 Hz, H-5), 3.67 (dd, 1H, *J* = 9.6, 6.3 Hz, H-5); ^{13}C-APT NMR ($CDCl_3$, 101 MHz, HSQC): δ 138.4, 138.1, 138.0 (C_q Bn), 135.2 (CH allyl), 128.6, 128.5, 128.4, 127.9, 127.9, 127.8, 127.7 (CH_{arom}), 116.9 (CH_2 allyl), 81.8 (C-2), 81.4 (C-3), 80.1 (C-1), 78.8 (C-4), 73.5, 72.4, 72.1 (CH_2 Bn), 68.5 (C-5), 33.7 (CH_2 allylic); ^{13}C HSQC-HECADE NMR ($CDCl_3$, 101 MHz): $^2J_{C1,H2}$ = +4.2 Hz, $^2J_{C2,H1}$ = +2.2 Hz, $^3J_{Callyl,H2}$ = +0.5 Hz; Diagnostic peaks for the β-anomer: ^{1}H NMR ($CDCl_3$, 400 MHz, HH-COSY, HSQC): δ 4.24 – 4.18 (m, 1H, H-4), 3.96 (dd, 1H, *J* = 3.9, 1.0 Hz, H-3), 3.92 (ddd, 1H, *J* = 7.1, 6.4, 3.5 Hz, H-1), 3.81 – 3.70 (m, 3H, H-2, H-5, H-5); ^{13}C-APT NMR ($CDCl_3$, 101 MHz, HSQC): δ 134.6 (CH allyl), 117.3 (CH_2 allyl), 85.9 (C-2), 83.4 (C-1), 83.0 (C-3), 80.1 (C-4), 73.6, 71.7, 71.7 (CH_2 Bn), 68.5 (C-5), 38.5 (CH_2 allylic); ^{13}C HSQC-HECADE NMR ($CDCl_3$, 101 MHz): $^2J_{C2,H1}$ = -4.0 Hz, $^3J_{Callyl,H2}$ = +4.5 Hz; HRMS: $[M+H]^+$ calcd for $C_{29}H_{33}O_4$ 445.23709, found 445.23734.

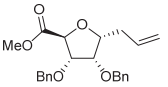

Methyl (1-allyl-2,3-di-*O*-benzyl-1-deoxy-α-D-ribofuranosyl uronate) (29). Donor **9** and allyltrimethylsilane (4 eq.) were condensed using the general procedure for furanosyl imidate glycosylations at -20°C for 100 h with TfOH as the promotor. Yield = 30.5 mg, 79 µmol, 79% as a white solid. R_f: 0.57 (4/1 pentane/EtOAc). $[\alpha]_D^{20}$ = +28.3° (*c* = 0.60, $CHCl_3$); IR (thin film): 698, 737, 916, 1026, 1099, 1144, 1206, 1275, 1356, 1454, 1748, 2868, 2922, 3030; ^{1}H NMR ($CDCl_3$, 500 MHz, HH-COSY, HSQC): δ 7.38 – 7.27 (m, 10H, CH_{arom}), 5.77 (ddt, 1H, *J* = 17.1, 10.2, 6.9 Hz, CH allyl), 5.11 (dq, 1H, *J* = 17.2, 1.6 Hz, C*H*H allyl), 5.04 (ddt, 1H, *J* = 10.2, 2.0, 1.1 Hz, CH*H* allyl), 4.82 (d, 1H, *J* = 11.6 Hz, C*H*H Bn), 4.67 (d, 1H, *J* = 12.0 Hz, C*H*H Bn), 4.63 (d, 1H, *J* = 12.0 Hz, CH*H* Bn), 4.59 (d, 1H, *J* = 6.0 Hz, H-4), 4.56 (d, 1H, *J* = 11.6 Hz, CH*H* Bn), 4.22 (dd, 1H, *J* = 6.0, 4.5 Hz, H-3), 4.17 (td, 1H, *J* = 7.0, 4.1 Hz, H-1), 3.99 (t, 1H, *J* = 4.3 Hz, H-2), 3.73 (s, 3H, CH_3CO_2Me), 2.56 – 2.48 (m, 2H, CH_2 allylic); ^{13}C-APT NMR ($CDCl_3$, 126 MHz, HSQC): δ 172.7 (C=O), 138.2, 137.6 (C_q), 134.6 (CH allyl), 128.6, 128.5, 128.1, 128.0, 127.9 (CH_{arom}), 117.3 (CH_2 allyl), 82.7 (C-3), 81.1 (C-1), 79.3 (C-4), 77.8 (C-2), 73.6, 72.8 (CH_2 Bn), 52.4 (CH_3CO_2Me), 34.0 (CH_2 allylic); ^{13}C HSQC-HECADE NMR ($CDCl_3$, 126 MHz): $^2J_{C2,H1}$: +1.5 Hz, $^3J_{Callyl,H2}$: +0.7 Hz; HRMS: $[M+NH_4]^+$ calcd for $C_{23}H_{30}NO_5$ 400.21185, found 400.21173.

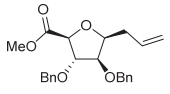

Methyl (1-allyl-2,3-di-*O*-benzyl-1-deoxy-β-D-arabinofuranosyl uronate) (30). Donor **10** and allyltrimethylsilane (4 eq.) were condensed using the general procedure for furanosyl imidate glycosylations at -20°C for 100 h with TfOH as the promotor. Yield = 29 mg, 76 µmol, 76% as a white solid (α:β = 5:95). R_f: 0.64 (4/1 pentane/EtOAc). $[\alpha]_D^{20}$ = +32.4° (*c* = 0.38, $CHCl_3$); IR (thin film): 698, 737, 916, 1028, 1101, 1207, 1279, 1454, 1726, 1761, 2920; ^{1}H NMR ($CDCl_3$, 500 MHz, HH-COSY, HSQC): δ 7.44 – 7.18 (m, 10H, CH_{arom}), 5.79 (ddt, 1H, *J* = 17.1, 10.2, 7.0 Hz, CH allyl), 5.14 (dq, 1H, *J* = 17.1, 1.5 Hz, C*H*H allyl), 5.08 – 5.02 (m, 1H, CH*H* allyl), 4.66 (d, 1H, *J* = 11.9 Hz, C*H*H Bn), 4.56 (d, 1H, *J* = 11.9 Hz, CH*H* Bn), 4.51 (d, 1H, *J* = 1.7 Hz, H-4), 4.49 (d, 1H, *J* = 11.8 Hz, C*H*H Bn), 4.39 – 4.34 (m, 2H, CH*H* Bn, H-3), 4.21 (td, 1H, *J* = 7.2, 3.5 Hz, H-1), 3.81 (dd, 1H, *J* = 3.5, 0.8 Hz, H-2), 3.68 (s, 3H, CH_3 CO_2Me), 2.64 – 2.50 (m, 2H, CH_2 allylic); ^{13}C-APT NMR ($CDCl_3$, 126 MHz, HSQC): δ 171.4 (C=O) 137.7, 137.5 (C_q), 134.7 (CH allyl), 128.6, 128.5, 128.1, 127.9, 127.9, 127.8 (CH_{arom}), 117.3 (CH_2 allyl), 85.2 (C-3), 82.4 (C-1), 81.6 (C-4), 81.3 (C-2), 71.9, 71.8 (CH_2 Bn), 52.3 (CO_2Me), 33.3 (CH_2 allylic); ^{13}C HSQC-HECADE NMR ($CDCl_3$, 126 MHz): $^2J_{C1,H2}$ = +2.5 Hz, $^2J_{C2,H1}$ = +2.5 Hz, $^3J_{Callyl,H2}$ = +0.3 Hz; HRMS: $[M+Na]^+$ calcd for $C_{23}H_{26}O_5Na$ 405.16725, found 405.16656.

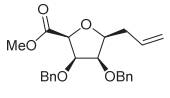

Methyl (1-allyl-2,3-di-*O*-benzyl-1-deoxy-β-D-lyxofuranosyl uronate) (31). Donor **11** and allyltrimethylsilane (4 eq.) were condensed using the general procedure for furanosyl imidate glycosylations at -20°C for 100 h with TfOH as the promotor. Yield = 29 mg, 76 µmol, 76% as a white solid. R_f: 0.32 (4/1 pentane/EtOAc). $[\alpha]_D^{20}$ = +3.6° (*c* = 0.58, $CHCl_3$); IR (thin film): 698, 737, 1028, 1072, 1084, 1099, 1152, 1207, 1356, 1437, 1454, 1732, 1763, 2870, 2920, 2949. ^{1}H NMR ($CDCl_3$, 500 MHz, HH-COSY, HSQC): δ 7.39 – 7.21 (m, 10H, CH_{arom}), 5.92 (ddt, 1H, *J* = 17.2, 10.2, 7.0 Hz, CH allyl), 5.15 (dq, 1H, *J* = 17.2, 1.4 Hz, C*H*H allyl), 5.09 – 5.04 (m, 1H, CH*H* allyl), 4.76 – 4.67 (m, 3H, CH_2 Bn, C*H*H Bn), 4.62 (d, 1H, *J* = 6.0 Hz, H-4), 4.56 (d, 1H, *J* = 11.8 Hz, CH*H* Bn), 4.34 (dd, 1H, *J* = 6.0, 4.4 Hz, H-3), 4.13 (dt, 1H, *J* = 8.8, 5.4 Hz, H-1), 4.04 (dd, 1H, *J* = 6.0, 4.4 Hz, H-2), 3.66 (s, 3H, CH_3 CO_2Me), 2.75 – 2.64 (m, 1H, C*H*H allylic), 2.58 – 2.48 (m, 1H, CH*H* allylic); ^{13}C-APT NMR ($CDCl_3$, 126 MHz, HSQC): δ 170.3 (C=O), 138.2, 138.2 (C_q), 135.8 (CH allyl), 128.5, 128.4, 127.8, 127.7, 127.6 (CH_{arom}), 116.8 (CH_2 allyl), 80.5 (C-1), 80.1 (C-3), 79.2 (C-2), 78.3 (C-4), 73.9, 73.2 (CH_2 Bn), 51.9 (CO_2Me), 35.0 (CH_2 allylic); ^{13}C HSQC-HECADE NMR ($CDCl_3$, 126 MHz): $^2J_{C2,H1}$ = -0.25 Hz, $^3J_{Callyl,H2}$ = +2.9 Hz; HRMS: $[M+NH_4]^+$ calcd for $C_{23}H_{30}NO_5$ 400.21185, found 400.21167.

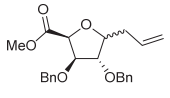

Methyl (1-allyl-2,3-di-*O*-benzyl-1-deoxy-α/β-D-xylofuranosyl uronate) (32). Donor **12** and allyltrimethylsilane (4 eq.) were condensed using the general procedure for furanosyl imidate glycosylations at -20°C for 100 h with TfOH as the promotor. Four fractions were isolated: amide **44** (1 mg, R_f: 0.66), mixed fraction (22 mg, product **32**, α:β = 35:65 as 68 wt%, and amide **44** as 32 wt%), title product **45** (7 mg, α:β = 69:33), cyclized product **61** (2 mg, R_f: 0.38) Calculated total title product yield = 22 mg, 57 µmol, 57%, (α:β = 45:55). R_f: 0.61 and 0.57 (4/1 pentane/EtOAc). Reported as a 1:1 mixture. IR (thin film): 698, 737, 1028, 1078, 1094, 1206, 1290, 1454, 1732, 1765, 2862, 2949. ^{1}H NMR ($CDCl_3$, 500 MHz, HH-COSY, HSQC): δ 7.38 – 7.24 (m, 20H, CH_{arom}), 5.88 – 5.72 (m, 2H, CH allyl), 5.16 – 5.03 (m, 4H, CH_2 allyl), 4.82 (d, 1H, *J* = 5.1 Hz, H-4α), 4.69 (d, 1H, *J* = 4.8 Hz, H-4β), 4.54 – 4.38 (m, 8H, 4xCH_2 Bn), 4.36 (ddd, 1H, *J* = 7.9, 6.5, 3.3 Hz, H-1α), 4.27 (dd, 1H, *J* = 5.1, 1.0 Hz, H-3α), 4.24 (dd, 1H, *J* = 4.8, 1.7 Hz, H-3β), 4.01 (td, 1H, *J* = 6.9, 3.3 Hz, H-1β), 3.82 (d, 1H, *J* = 3.5 Hz, H-2α), 3.82 (d, 1H, *J* = 3.4 Hz, H-2β), 3.76 (s, 3H, CH_3 CO_2Meβ), 3.73 (s, 3H, CH_3 CO_2Meα), 2.64 – 2.41 (m, 4H, CH2 allylic); ^{13}C-APT NMR ($CDCl_3$, 126 MHz, HSQC): δ 170.6 (C=Oα), 169.6 (C=Oβ), 137.7 ($C_{qα}$), 137.7 ($C_{qβ}$), 137.6 ($C_{qβ}$), 137.5 ($C_{qα}$), 134.5 (CH allylα), 134.4 (CH allylβ), 128.6, 128.6, 128.6, 128.6, 128.1, 128.1, 128.1, 127.9, 127.9, 127.9 (CH_{arom}), 117.6 (CH_2 allylicβ), 117.3 (CH_2 allylicα), 84.7 (C-2β), 84.0 (C-1β), 83.9 (C-3β), 82.9 (C-3α), 81.6 (C-1α), 81.4 (C-2α), 80.4 (C-4β), 80.0 (C-4α), 73.0, 72.5, 72.3, 72.0 (CH_2 Bn), 52.1 (CO_2Meβ), 52.0 (CO_2Meα), 38.1 (CH_2 allylicβ), 33.1 (CH_2 allylicα); ^{13}C HSQC-HECADE NMR ($CDCl_3$, 126 MHz): α-anomer: $^2J_{C1,H2}$ = +1.5 Hz, $^2J_{C2,H1}$ = +2.4 Hz, $^3J_{Callyl,H2}$ = +0.2 Hz, β-anomer: $^2J_{C1,H2}$ = -1.5 Hz, $^2J_{C2,H1}$ = -4.5 Hz, $^3J_{Callyl,H2}$ = +2.9 Hz; HRMS: $[M+NH_4]^+$ calcd for $C_{23}H_{30}NO_5$ 400.21185, found 400.21153.

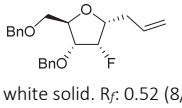

Allyl 3,5-di-*O*-benzyl-1,2-dideoxy-2-fluoro-α-D-ribofuranoside (33). Donor **13** and allyltrimethylsilane (4 eq.) were condensed using the general procedure for furanosyl imidate glycosylations at -20°C for 100 h with TfOH as the promotor. Yield = 27 mg, 76 µmol, 76% as a white solid. R_f: 0.52 (8/2 pentane/Et_2O). Spectroscopic data were in accord with those previously reported.[13] ^{1}H NMR ($CDCl_3$, 500 MHz, HH-COSY, HSQC): δ 7.40 – 7.19 (m, 10H, CH_{arom}), 5.80 (ddtd, 1H, *J* = 17.3, 10.2, 7.0, 0.8 Hz, CH allyl), 5.20 – 5.14 (m, 1H, C*H*H allyl), 5.09 (ddt, 1H, *J* = 10.2, 2.1, 1.1 Hz, CH*H* allyl), 4.89 (dt, 1H, *J* = 55.2, 2.9 Hz, H-2), 4.69 (d, 1H, *J* = 11.7 Hz, C*H*H Bn), 4.59 (d, 1H, *J* = 12.1 Hz, C*H*H Bn), 4.52 (d, 1H, *J* = 11.7 Hz, CH*H* Bn), 4.49 (d, 1H, *J* = 12.1 Hz, CH*H* Bn), 4.21 – 4.16 (m, 1H, H-4), 4.11 (ddd, 1H, *J* = 8.6, 3.5, 0.5 Hz, H-3), 4.05 (dtd, 1H, *J* = 29.3, 7.4, 2.4 Hz, H-1), 3.71 (dd, 1H, *J* = 10.8, 2.4 Hz, H-5), 3.56 (dd, 1H, *J* = 10.9, 3.4 Hz, H-5), 2.49 (ddt, 2H, *J* = 7.0, 5.6, 1.4 Hz, CH_2 allylic); ^{13}C-APT NMR ($CDCl_3$, 126 MHz, HSQC): δ 138.3, 137.6 (C_q), 133.6 (CH allyl), 128.6, 128.5, 128.1, 128.0, 127.8, 127.7

(CH_{arom}), 118.0 (CH allyl), 90.1 (d, *J* = 191.0 Hz, C-2), 80.0 (d, *J* = 18.3 Hz, C-1), 79.2 (C-4), 78.6 (d, *J* = 16.5 Hz, C-3), 73.6, 72.5 (CH_2 Bn), 69.6 (C-5), 33.7 (d, *J* = 9.3 Hz, CH allylic); ^{19}F NMR ($CDCl_3$, 471 MHz): δ -215.30 (ddd, *J* = 53.7, 29.4, 23.5 Hz, F-2); ^{13}C HSQC-HECADE NMR ($CDCl_3$, 126 MHz): $^2J_{C2,H1}$ = +4.9 Hz, $^3J_{Callyl,H2}$ = +0.2 Hz; HRMS: $[M+NH_4]^+$ calcd for $C_{22}H_{29}FNO_3$ 374.21260, found 374.21252.

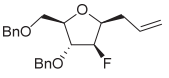

Allyl 3,5-di-*O*-benzyl-1,2-dideoxy-2-fluoro-β-D-arabinofuranoside (34). Donor **14** and allyltrimethylsilane (4 eq.) were condensed using the general procedure for furanosyl imidate glycosylations at -20°C for 100 h with TfOH as the promotor. Yield = 28 mg, 79 µmol, 79% as a colourless oil. R_f: 0.80 (9/1 pentane/EtOAc). $[\alpha]_D^{20}$ = -29.7° (*c* = 0.93, $CHCl_3$); IR (thin film):700, 712, 1026, 1070, 1096, 1269, 1452, 2924; ^{1}H NMR ($CDCl_3$, 500 MHz, HH-COSY, HH-NOESY, HSQC): δ 7.36 – 7.25 (m, 10H, CH_{arom}), 5.84 (ddtd, 1H, *J* = 17.2, 10.2, 7.1, 0.7 Hz, CH allyl), 5.17 (dq, 1H, *J* = 17.1, 1.5 Hz, C*H*H allyl), 5.10 (ddt, 1H, *J* = 10.2, 2.0, 1.1 Hz, CH*H* allyl), 4.88 (dd, 1H, *J* = 52.0, 2.8 Hz, H-2), 4.66 – 4.53 (m, 4H, 2xCH_2 Bn), 4.04 – 3.98 (m, 2.5H, H-1, H-3, H-4), 3.95 (td, 0.5H, *J* = 7.2, 2.8 Hz, H-3), 3.65 – 3.59 (m, 1H, H-5), 3.56 – 3.51 (m, 1H, H-5), 2.55 – 2.42 (m, 2H, CH_2 allylic);^{13}C-APT NMR ($CDCl_3$, 126 MHz, HSQC): δ 138.2, 137.4 (C_q), 133.8 (CH allyl), 128.6, 128.5, 128.1, 127.9, 127.9, 127.8 (CH_{arom}), 117.8 (CH_2 allyl), 95.89 (d, *J* = 186.6 Hz, C-2), 84.71 (d, *J* = 27.3 Hz, C-3), 82.5 (C-4), 80.70 (d, *J* = 20.9 Hz, C-1), 73.6, 72.2 (CH_2 Bn), 70.2 (C-5), 32.63 (d, *J* = 8.1 Hz, CH_2 allylic); ^{19}F NMR ($CDCl_3$, 471 MHz): δ -198.80 (ddd, *J* = 50.6, 29.6, 20.2 Hz); ^{13}C HSQC-HECADE NMR ($CDCl_3$, 126 MHz): $^2J_{C1,H2}$ = +4.2 Hz, $^2J_{C2,H1}$ = +5.6 Hz, $^3J_{Callyl,H2}$ = 0.1 Hz; HRMS: $[M+NH_4]^+$ calcd for $C_{22}H_{29}FNO_3$ 374.21260, found 374.21280.

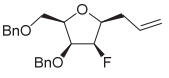

Allyl 3,5-di-*O*-benzyl-1,2-dideoxy-2-fluoro-β-D-lyxofuranoside (35). Donor **15** and allyltrimethylsilane (4 eq.) were condensed using the general procedure for furanosyl imidate glycosylations at -20°C for 100 h with TfOH as the promotor. Yield = 32 mg, 90 µmol, 90% as a white solid. R_f: 0.28 (9/1 pentane/EtOAc). $[\alpha]_D^{20}$ = -10.5° (*c* = 1.07, $CHCl_3$); IR (thin film): 696, 711, 737, 1026, 1070, 1271, 1452, 2870, 2922; ^{1}H NMR ($CDCl_3$, 500 MHz, HH-COSY, HSQC): δ 7.42 – 7.21 (m, 10H, CH_{arom}), 5.82 (ddt, 1H, *J* = 17.2, 10.2, 7.0 Hz, CH allyl), 5.17 (dd, 1H, *J* = 17.1, 1.5 Hz, C*H*H allyl), 5.12 – 5.06 (m, 1H, CH*H* allyl), 4.89 (ddd, 1H, *J* = 54.6, 4.0, 2.9 Hz, H-2), 4.69 (d, 1H, *J* = 11.9 Hz, C*H*H Bn), 4.62 (d, 1H, *J* = 12.2 Hz, C*H*H Bn), 4.58 – 4.51 (m, 2H, 2xCH*H* Bn), 4.28 (td, 1H, *J* = 7.7, 3.6 Hz, H-4), 4.19 (ddd, 1H, *J* = 22.8, 7.8, 4.0 Hz, H-3), 3.84 (dtd, 1H, *J* = 27.3, 7.2, 2.8 Hz, H-1), 3.80 (dd, 1H, *J* = 10.6, 3.7 Hz, H-5), 3.65 (ddd, 1H, *J* = 10.6, 7.7, 1.7 Hz, H-5), 2.51 (t, 2H, *J* = 7.1 Hz, CH_2 allylic); ^{13}C-APT NMR ($CDCl_3$, 126 MHz, HSQC): δ 138.6, 137.5 (C_q), 133.7 (CH allyl), 128.6, 128.4, 128.1, 127.9, 127.8, 127.6 (CH_{arom}), 117.9 (CH_2 allyl), 90.2 (d, *J* = 193.1 Hz, C-2), 79.3 (d, *J* = 18.8 Hz, C-1), 78.6 (d, *J* = 15.7 Hz, C-3), 78.2 (C-4), 73.5, 72.8 (CH_2 Bn), 70.6 (d, *J* = 2.7 Hz, C-5), 33.9 (d, *J* = 8.1 Hz, CH_2 allylic); ^{19}F NMR ($CDCl_3$, 471 MHz): δ -213.57 (ddd, *J* = 54.5, 27.2, 22.9 Hz); ^{13}C HSQC-HECADE NMR ($CDCl_3$, 126 MHz): $^2J_{C1,H2}$ = +1.2 Hz, $^2J_{C2,H1}$ = +5.2 Hz, $^3J_{Callyl,H2}$ = +0.4 Hz; HRMS: $[M+NH_4]^+$ calcd for $C_{22}H_{29}FNO_3$ 374.21260, found 374.21295.

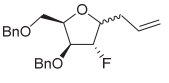

Allyl 3,5-di-*O*-benzyl-1,2-dideoxy-2-fluoro-α/β-D-xylofuranoside (36). Donor **16** and allyltrimethylsilane (4 eq.) were condensed using the general procedure for furanosyl imidate glycosylations at -20°C for 100 h with TfOH as the promotor. Yield = 22 mg, 62 µmol, 62% as a colourless oil (α:β = 70:30), and 12 mg (24%) of the anomeric amide (**42**). R_f: 0.53 and 0.40 (9/1 pentane/Et_2O). IR (thin film): 696, 735, 1028, 1076, 1088, 1454, 2868, 2922; ^{1}H NMR ($CDCl_3$, 500 MHz, HH-COSY, HSQC): δ 7.37 – 7.25 (m, 10H, CH_{arom}), 5.88 – 5.77 (m, 1H, CH allyl), 5.19 – 5.07 (m, 2H, CH_2 allyl), 4.91 (ddd, 0.7H, *J* = 51.4, 2.8, 1.3 Hz, H-2α), 4.79 (ddd, 0.3H, *J* = 52.6, 2.9, 1.4 Hz, H-2β), 4.65 (d, 0.3H, *J* = 11.9 Hz, C*H*H Bnβ), 4.65 – 4.58 (m, 1.7H, 2xC*H*H Bnα, C*H*H Bnβ), 4.56 (d, 0.7H, *J* = 11.9 Hz, CH*H* Bnα), 4.53 – 4.49 (m, 1.3H, 2xCH*H* Bnβ, CH*H* Bnα), 4.42 – 4.36 (m, 0.7H, H-4α), 4.26 – 4.12 (m, 1.7H, H-1α, H-3α, H-4β), 4.08 (ddd, 0.3H, *J* = 8.9, 4.3, 1.3 Hz, H-3β), 4.02 (dddd, 0.3H, *J* = 13.9, 7.3, 6.5, 2.8 Hz, H-1β), 3.76 (dd, 0.3H, *J* = 10.0, 5.3 Hz, H-5β), 3.73 – 3.69 (m, 1H, H-5α, H-5β), 3.67 (dd, 0.7H, *J* = 9.8, 6.4 Hz, H-5α), 2.54 – 2.36 (m, 2H, CH_2 allylic); ^{13}C-APT NMR ($CDCl_3$, 126 MHz, HSQC): δ 138.3, 138.2, 137.6 (C_q), 134.0 (CH allylα), 133.8 (CHallylβ), 128.6, 128.6, 128.5, 128.1, 128.0, 127.9, 127.9, 127.8, 127.7, 127.7, 127.7 (CH_{arom}), 117.8 (CH_2 allylβ), 117.7 (CH_2 allylα), 97.7 (d, *J* = 182.9 Hz, C-2β), 94.4 (d, *J* = 187.9 Hz, C-2α), 82.4 (d, *J* = 35.5 Hz, C-3β), 82.4 (d, *J* = 13.9 Hz, C-1β), 81.8 (d, *J* = 25.8 Hz, C-3α), 79.8 (d, *J* = 1.6 Hz, C-4β), 79.6 (d, *J* = 19.0 Hz, C-1α), 78.9 (C-4α), 73.6 (CH_2 Bnβ), 73.6, 72.9 (CH_2 Bnα), 72.1 (CH_2 Bnβ), 68.3 (C-5β), 68.2 (C-5α), 37.4 (d, *J* = 7.6 Hz, CH_2 allylicβ), 33.1 (d, *J* = 10.3 Hz, CH_2 allylicα); ^{19}F NMR ($CDCl_3$, 471 MHz): δ -183.53 (dddd, 0.3F, *J* = 52.6, 28.0, 13.2, 1.8 Hz), -201.43 (dddd, 0.7F, *J* = 51.4, 31.9, 9.9, 2.5 Hz); ^{13}C HSQC-HECADE NMR ($CDCl_3$, 126 MHz): α-anomer: $^2J_{C1,H2}$ = +5.0 Hz, $^2J_{C2,H1}$ = +4.5 Hz, $^3J_{Callyl,H2}$ = +0.3 Hz, β-anomer: $^2J_{C1,H2}$ = +1.3 Hz, $^2J_{C2,H1}$ = -5.4 Hz, $^3J_{Callyl,H2}$ = +2.8 Hz; HRMS: $[M+Na]^+$ calcd for $C_{22}H_{25}FO_3Na$ 379.1685, found 379.1685.

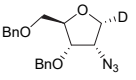

1-[^{2}H]-1,4-anhydro-2-azido-3,5-di-*O*-benzyl-2-deoxy-α-D-ribitol (37). Donor **17** and triethylsilane-*d* (4 eq.) were condensed using the general procedure for furanosyl imidate glycosylations at 0-5°C for 100 h with TfOH as the promotor. Yield = 23 mg, 68 µmol, 68% as a colourless oil. Inseparable mixture of **37** and amide **46** (in a 95:5 ratio). R_f: 0.26 (9/1 pentane/EtOAc). $[\alpha]_D^{20}$ = +88° (*c* = 0.77, $CHCl_3$) IR (thin film): 698, 738, 1028, 1089, 1269, 1454, 2104, 2864; ^{1}H NMR ($CDCl_3$, 500 MHz, HH-COSY, HH-NOESY, HSQC): δ 7.38 – 7.26 (m, 10H, CH_{arom}), 4.69 (d, 1H, *J* = 11.8 Hz, C*H*H Bn), 4.57 – 4.52 (m, 2H, C*H*H Bn, CH*H* Bn), 4.48 (d, 1H, *J* = 12.0 Hz, CH*H* Bn), 4.14 (dd, 1H, *J* = 6.1, 5.5 Hz, H-3), 4.09 – 4.02 (m, 2H, H-1, H-4), 3.89 (t, 1H, *J* = 5.4 Hz, H-2), 3.61 (dd, 1H, *J* = 10.7, 3.3 Hz, H-5), 3.50 (dd, 1H, *J* = 10.7, 4.0 Hz, H-5); ^{13}C-APT NMR ($CDCl_3$, 126 MHz, HSQC): δ 138.1, 137.4 (C_q), 128.6, 128.5, 128.2, 128.1, 127.8, 127.8 (CH_{arom}), 80.9 (C-4), 79.9 (C-3), 73.6, 73.0 (CH_2 Bn), 70.2 (t, *J* =22.8 Hz, C-1), 69.8 (C-5), 60.8 (C-2); ^{2}H NMR ($CHCl_3$, 77 MHz): δ 3.90; ^{13}C HSQC-HECADE NMR ($CDCl_3$, 126 MHz): $^2J_{C1\text{-}H2}$: +1.5 Hz, $^2J_{C2\text{-}H1}$: +1.3 Hz; HRMS: $[M+Na]^+$ calcd for $C_{19}H_{20}DN_3O_3Na$ 363.1543, found 363.1546.

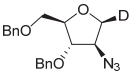

1-[^{2}H]-1,4-anhydro-2-azido-3,5-di-*O*-benzyl-2-deoxy-β-D-arabitol (38). Donor **18** and triethylsilane-*d* (4 eq.) were condensed using the general procedure for furanosyl imidate glycosylations at 0-5°C for 100 h with TfOH as the promotor. Yield = 19.5 mg, 57 µmol, 57% as a colourless oil. R_f: 0.38 (9/1 pentane/EtOAc). Spectroscopic data were in accord with those previously reported for the non-deuterated compound.[37] $[\alpha]_D^{20}$ = -14.6° (*c* = 0.98, $CHCl_3$); IR ^{1}H NMR ($CDCl_3$, 500 MHz, HH-COSY, HSQC): δ 7.37 – 7.26 (m, 10H, CH_{arom}), 4.59 (d, 1H, *J* = 11.8 Hz, C*H*H Bn), 4.56 (s, 2H, CH_2 Bn), 4.54 (d, 1H, *J* = 11.8 Hz, CH*H* Bn), 4.02 (td, 1H, *J* = 5.3, 4.3 Hz, H-4), 4.00 (bs, 1H, H-1), 3.98 (dd, 1H, *J* = 5.0, 1.9 Hz, H-2), 3.92 (dd, 1H, *J* = 4.3, 1.9 Hz, H-3), 3.59 (dd, 1H, *J* = 10.3, 5.5 Hz, H-5), 3.57 (dd, 1H, *J* = 10.3, 5.2 Hz, H-5); ^{13}C-APT NMR ($CDCl_3$, 126 MHz, HSQC): δ 138.1, 137.4 (C_q), 128.7, 128.5, 128.2, 128.0, 127.9, 127.8 (CH_{arom}), 85.0 (C-3), 83.4 (C-4), 73.6, 72.4 (CH_2 Bn), 70.7 (t, *J* = 23.0 Hz, C-1), 70.5, 70.0 (C-5), 65.9 (C-2); ^{2}H NMR ($CHCl_3$, 77 MHz): δ 4.02; ^{13}C HSQC-HECADE NMR ($CDCl_3$, 126 MHz): $^2J_{C1\text{-}H2}$: +1.1 Hz, $^2J_{C2\text{-}H1}$: +2.3 Hz; HRMS: $[M+NH_4]^+$ calcd for $C_{19}H_{24}DN_4O_3$ 358.19839, found 358.19858.

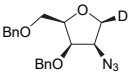

1-[^{2}H]-1,4-anhydro-2-azido-3,5-di-*O*-benzyl-2-deoxy-β-D-lyxitol (39). Donor **19** and triethylsilane-*d* (4 eq.) were condensed using the general procedure for furanosyl imidate glycosylations at 0-5°C for 100 h with TfOH as the promotor. Yield = 20 mg, 59 µmol, 59% as a colourless oil. R_f: 0.13 (9/1 pentane/EtOAc). $[\alpha]_D^{20}$ = -37° (*c* = 1.0, $CHCl_3$); IR (thin film): 698, 738, 1984, 1269, 1452, 2104, 2868, 2922, 3032; ^{1}H NMR ($CDCl_3$, 500 MHz, HH-COSY, HSQC): δ 7.36 – 7.26 (m, 10H, CH_{arom}), 4.77 (d, 1H, *J* = 11.6 Hz, C*H*H Bn), 4.61 – 4.56 (m, 2H, C*H*H Bn, CH*H* Bn), 4.50 (d, 1H, *J* = 11.9 Hz, CH*H* Bn), 4.20 (t, 1H, *J* = 5.2 Hz, H-3), 4.15 (dt, 1H, *J* = 6.9, 5.2 Hz, H-4), 3.92 (d, 1H, *J* = 6.4 Hz, H-1), 3.86 (dd, 1H, *J* = 6.3, 5.1 Hz, H-2), 3.73 (dd, 1H, *J* = 10.1, 5.0 Hz, H-5), 3.68 (dd, 1H, *J* = 10.1, 7.0 Hz, H-5); ^{13}C-APT NMR ($CDCl_3$, 126 MHz, HSQC): δ 138.2, 137.5 (C_q), 128.6, 128.5, 128.1, 128.0, 127.9, 127.8 (CH_{arom}), 79.6, 79.6 (C-3, C-4), 74.0, 73.7 (CH_2 Bn), 69.0 (C-5), 68.7 (t, *J* = 22.8 Hz, C-1), 61.3 (C-2); ^{2}H NMR ($CHCl_3$, 77 MHz): δ 3.95; ^{13}C HSQC-HECADE NMR: $^2J_{C2,H1}$ = +0.2 Hz; HRMS: $[M+Na]^+$ calcd for $C_{19}H_{20}DN_3O_3Na$ 363.1543, found 363.1551.

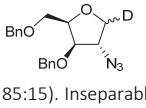

1-[^{2}H]-1,4-anhydro-2-azido-3,5-di-*O*-benzyl-2-deoxy-α/β-D-xylitol (40). Donor **20** and triethylsilane-*d* (4 eq.) were condensed using the general procedure for furanosyl imidate glycosylations at 0-5°C for 100 h with TfOH as the promotor. Yield = 23 mg, 68 µmol, 68% as a colourless oil (α:β = 85:15). Inseparable mixture of **40** and amide **43** (in a 73:27 ratio) R_f: 0.30 (85/15 pentane/Et_2O). IR (thin film): 696, 735, 1061, 1088, 1207, 1454, 1494, 1690, 2106, 2916; ^{1}H NMR ($CDCl_3$, 500 MHz, HH-COSY, HSQC): δ 7.38 – 7.24 (m, 10H, CH_{arom}), 4.65 – 4.58 (m, 2H, 2x*CH*H Bn), 4.54 (d, 1H, *J* = 11.9 Hz, CH*H* Bn), 4.52 (d, 1H, *J* = 11.9 Hz, CH*H* Bn), 4.21 – 4.15 (m, 1.85H, H-1α, H-4), 4.04 (dd, 1H, *J* = 5.5, 1.9 Hz, H-2), 3.99 (dd, 1H, *J* = 4.4, 1.9 Hz, H-3), 3.74 – 3.70 (m, 1.15H, H-1β, H-5), 3.68 (dd, 1H, *J* = 10.0, 6.4 Hz, H-5); ^{13}C-APT NMR ($CDCl_3$, 126 MHz, HSQC): δ 138.2, 137.4 (C_q), 128.7, 128.5, 128.2, 127.9, 127.8, 127.8 (CH_{arom}), 82.9 (C-3), 79.7 (C-4), 73.7, 72.6 (CH_2 Bn), 70.0 (t, *J* = 22.7 Hz C-1β), 70.0 (t, *J* = 22.7, C-1α) 68.4 (C-5), 65.0 (C-2); ^{2}H NMR ($CHCl_3$, 77 MHz): δ 4.19 (s, 0.15H), 3.75 (s, 0.85H);^{13}C HSQC-HECADE NMR ($CDCl_3$, 126 MHz): α-anomer: $^2J_{C2,H1}$ = +0.7 Hz; β-anomer: $^2J_{C2,H1}$ = -4.3 Hz; HRMS: $[M+Na]^+$ calcd for $C_{19}H_{20}DN_3O_3Na$ 363.1543, found 363.1549.

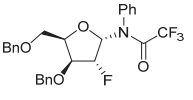

3,5-di-*O*-benzyl-1,2-dideoxy-2-fluoro-1-*N*-[phenyl]trifluoroacetyl-α/β-D-xylofuranoside (42). IR (thin film): 698, 737, 1070, 1153, 1188, 1207, 1454, 1495, 1595, 1690, 2862, 2922; ^{1}H NMR ($CDCl_3$, 500 MHz, HH-COSY, HSQC): δ 7.43 – 7.19 (m, 15H, CH_{arom}), 6.31 (dd, 1H, *J* = 11.0, 5.1 Hz, H-1), 5.45 (ddd, 1H, *J* = 52.9, 5.0, 3.8 Hz, H-2), 4.65 (d, 1H, *J* = 11.9 Hz, C*H*H Bn), 4.47 (d, 1H, *J* = 11.9 Hz, CH*H* Bn), 4.40 (s, 2H, CH_2 Bn), 3.91 (dt, 1H, *J* = 14.3, 4.1 Hz, H-3), 3.77 (qd, 1H, *J* = 4.7, 1.7 Hz, H-4), 3.56 (ddd, 1H, *J* = 10.5, 4.4, 0.7 Hz, H-5), 3.49 (dd, 1H, *J* = 10.6, 4.8 Hz, H-5); ^{13}C-APT NMR ($CDCl_3$, 101 MHz, HSQC): δ 138.0, 137.1 (C_q), 134.2, 132.0, 130.5, 129.6, 128.6, 128.5, 128.2, 127.9, 127.8, 127.7 (CH_{arom}), 93.5 (d, *J* =

194.8 Hz, C-2), 87.2 (d, *J* = 17.4 Hz, C-1), 80.1 (d, *J* = 23.2 Hz, C-3), 79.1 (d, *J* = 3.5 Hz, C-4), 73.4, 72.6 (CH_2 Bn), 68.0 (C-5); ^{19}F NMR ($CDCl_3$, 471 MHz): δ -68.17 (s, 3F, CF_3), -196.37 (dt, 1F, *J* = 53.1, 12.7 Hz, F-2).

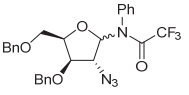

2-azido-3,5-di-*O*-benzyl-1,2-dideoxy-1-*N*-[phenyl]trifluoroacetyl-α/β-D-xylofuranoside (43). Intermixed with **40**. The anomeric amide was formed in an α:β = 93:7 ratio. Data for the α-anomer: ^1H NMR ($CDCl_3$, 500 MHz, HH-COSY, HSQC): δ 7.17 (dd, 2H, *J* = 6.6, 2.6 Hz, NPh), 6.33 (d, 1H, *J* = 6.6 Hz, H-1), 4.59 (t, 1H, *J* = 6.6 Hz, H-2), 4.50 (d, 1H, *J* = 11.7 Hz, C*H*H Bn), 4.46 – 4.40 (m, 3H, CH_2 Bn, CH*H* Bn), 3.66 (t, 1H, *J* = 4.3 Hz, H-4), 3.59 (t, 1H, *J* = 6.8 Hz, H-3), 3.49 (dd, 1H, *J* = 10.7, 4.0 Hz, H-5), 3.41 (dd, 1H, *J* = 10.7, 4.5 Hz, H-5); ^{13}C-APT NMR ($CDCl_3$, 126 MHz, HSQC): δ 157.0 (q, *J* = 36.4 Hz, F_3C-*C*=O), 138.0, 137.0 (C_q), 132.0, 130.7, 129.6, 129.5, 128.7, 128.3, 128.1, 127.8, 127.8, 127.7, 126.5, 120.6 (CH_{arom}), 116.0 (q, *J* = 288.7 Hz, CF_3), 86.9 (C-1), 80.9 (C-3), 78.6 (C-4), 73.5, 73.3 (CH_2 Bn), 68.6 (C-5), 67.1 (C-2); ^{19}F NMR ($CDCl_3$, 471 MHz): δ -68.04 (s, $CF_{3,\alpha}$), -68.18 (s, $CF_{3,\beta}$); ^{13}C HSQC-HECADE NMR ($CDCl_3$, 126 MHz): α-anomer: $^2J_{C1,H2}$ = -0.2 Hz, $^2J_{C2,H1}$ = +1.1 Hz; Diagnostic peaks for the β-anomer: ^1H NMR ($CDCl_3$, 500 MHz, HH-COSY, HSQC): 5.98 (d, 0.07H, *J* = 6.2 Hz, H-1), 4.28 (td, 0.07H, *J* = 6.3, 4.6 Hz, H-4); ^{13}C HSQC-HECADE NMR: $^2J_{C1,H2}$ = -4.0 Hz, $^2J_{C2,H1}$ = -2.1 Hz.

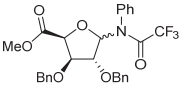

Methyl (2,3-di-*O*-benzyl-1-deoxy-1-*N*-[phenyl]trifluoroacetyl-α/β-D-xylofuranosyl uronate) (44). ^1H NMR ($CDCl_3$, 500 MHz, HH-COSY, HH-NOESY, HSQC, HMBC): δ 7.41 – 7.28 (m, 18H, CH_{arom}), 7.15 (dd, 2H, *J* = 7.3, 2.0 Hz, CH_{arom}), 6.59 (d, 1H, *J* = 6.1 Hz, H-1), 4.70 (d, 1H, *J* = 11.2 Hz, C*H*H Bn), 4.58 (d, 1H, *J* = 11.2 Hz, CH*H* Bn), 4.51 (t, 1H, *J* = 6.1 Hz, H-2), 4.44 (d, 1H, *J* = 11.7 Hz, C*H*H Bn), 4.38 (d, 1H, *J* = 11.9 Hz, CH*H* Bn), 4.15 (d, 1H, *J* = 6.5 Hz, H-4), 3.77 – 3.72 (m, 1H, H-3), 3.67 (s, 3H, CH_3 CO_2Me); ^{13}C-APT NMR ($CDCl_3$, 126 MHz, HSQC, HMBC): δ 169.5 (C=O), 137.3, 137.1 (C_q), 129.6, 128.7, 128.6, 128.5, 128.3, 128.2, 128.1, 127.9 (CH_{arom}), 87.6 (C-1), 81.9 (C-2), 81.1 (C-3), 78.2 (C-4), 74.3, 72.9 (CH_2 Bn), 52.3 (CO_2Me); ^{19}F NMR ($CDCl_3$, 471 MHz): δ -68.09; ^{13}C HSQC-HECADE NMR ($CDCl_3$, 126 MHz): $^2J_{C1,H2}$ = +1.5 Hz.

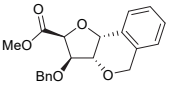

Methyl (2*S*,3*R*,3a*S*,9b*R*)-3-(benzyloxy)-3,3a,5,9b-tetrahydro-2*H*-furo[3,2-*c*]isochromene-2-carboxylate (45). ^1H NMR ($CDCl_3$, 500 MHz, HH-COSY, HH-NOESY, HSQC): δ 7.61 – 7.57 (m, 1H, CH_{arom}), 7.37 – 7.28 (m, 7H, CH_{arom}), 7.08 – 7.04 (m, 1H, CH_{arom}), 5.16 (d, 1H, *J* = 2.8 Hz, H-1), 4.92 (d, 1H, *J* = 4.9 Hz, H-4), 4.78 (d, 1H, *J* = 14.6 Hz, C*H*H Bn $_{(C\text{-}2)}$), 4.72 (d, 1H, *J* = 11.9 Hz, C*H*H Bn $_{(C\text{-}3)}$), 4.65 (d, 1H, *J* = 14.8 Hz, CH*H* Bn $_{(C\text{-}2)}$), 4.64 (d, 1H, *J* = 12.0 Hz, CH*H* Bn $_{(C\text{-}3)}$), 4.44 (d, 1H, *J* = 5.1 Hz, H-3), 4.26 (d, 1H, *J* = 3.0 Hz, H-2), 3.76 (s, 3H, CH_3 CO_2Me); ^{13}C-APT NMR ($CDCl_3$, 126 MHz, HSQC): δ 170.2 (C=O), 134.4, 130.9, 130.3 (C_q), 128.7, 128.6, 128.1, 127.7, 127.7, 124.2 (CH_{arom}), 85.2 (C-3), 80.4 (C-4), 79.5 (C-2), 74.9 (C-1), 73.2 (CH_2 $Bn_{(C\text{-}3)}$), 67.2 (CH_2 $Bn_{(C\text{-}2)}$), 52.1 (CO_2Me).

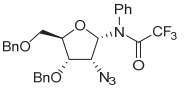

3,5-di-*O*-benzyl-1,2-dideoxy-2-fluoro-1-*N*-[phenyl]trifluoroacetyl-α-D-ribofuranoside (46). Intermixed with **37**. Diagnostic peaks: ^1H NMR ($CDCl_3$, 500 MHz): δ 6.04 (d, 1H, *J* = 5.1 Hz, H-1), 4.61 (t, 1H, *J* = 5.5 Hz, H-2), 4.44 (d, 1H, *J* = 11.6 Hz, C*H*H Bn), 4.41 (d, 1H, *J* = 12.0 Hz, C*H*H Bn), 4.30 (d, 1H, *J* = 12.0 Hz, CH*H* Bn), 3.44 (dd, 1H, *J* = 11.3, 2.5 Hz, H-5), 3.32 (dd, 1H, *J* = 11.3, 3.5 Hz, H-5); ^{13}C-APT NMR ($CDCl_3$, 126 MHz, HSQC): δ 88.1 (C-1), 80.3 (C-4), 77.0 (C-3), 73.4, 73.3 (CH_2 Bn), 68.0 (C-5), 62.9 (C-2).

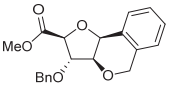

Methyl (2*S*,3*S*,3a*R*,9b*S*)-3-(benzyloxy)-3,3a,5,9b-tetrahydro-2*H*-furo[3,2-*c*]isochromene-2-carboxylate (47). Intermixed with **30**. ^1H NMR ($CDCl_3$, 500 MHz, HH-COSY, HSQC): δ 7.52 (dd, 1H, *J* = 5.5, 3.6 Hz, CH_{arom}), 7.44 – 7.25 (m, 7H, CH_{arom}), 7.07 (dd, 1H, *J* = 5.4, 3.8 Hz, CH_{arom}), 4.93 (d, 1H, *J* = 2.9 Hz, H-1), 4.79 (d, 1H, *J* = 12.1 Hz, C*H*H 3-OBn), 4.79 (d, 1H, *J* = 14.7 Hz, C*H*H 2-OBn), 4.72 (d, 1H, *J* = 12.1 Hz, CH*H* 3-OBn), 4.66 (d, 1H, *J* = 14.7 Hz, CH*H* 2-OBn), 4.64 (d, 1H, *J* = 2.8 Hz, H-4), 4.46 (dd, 1H, *J* = 2.7, 0.7 Hz, H-3), 4.21 (d, 1H, *J* = 3.0 Hz, H-2), 3.71 (s, 3H, CH_3 CO_2Me); ^{13}C-APT NMR ($CDCl_3$, 126 MHz, HSQC): δ 170.6 (C=O), 137.4, 134.7, 130.7 (C_q), 129.8, 128.7, 128.1, 128.0, 128.0, 127.5, 124.2 (CH_{arom}), 87.8 (C-3), 82.2 (C-4), 79.8 (C-2), 75.3 (C-1), 72.4, 67.0 (CH_2 Bn), 52.4 (CO_2Me); ^{13}C HSQC-HECADE NMR ($CDCl_3$, 126 MHz): $^2J_{C1,H2}$ = +6.0 Hz, $^2J_{C2,H1}$ = +2.4 Hz.

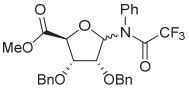

Methyl (2,3-di-*O*-benzyl-1-deoxy-1-*N*-[phenyl]trifluoroacetyl-α-D-ribofuranosyl uronate) (48). ^1H NMR ($CDCl_3$, 400 MHz, HH-COSY, HSQC): δ 7.43 – 7.16 (m, 14H, CH_{arom}), 7.09 – 7.00 (m, 1H, NPh), 6.44 (d, 1H, *J* = 5.8 Hz, H-1), 4.75 (d, 1H, *J* = 11.1 Hz, C*H*H Bn), 4.65 (d, 1H, *J* = 11.0 Hz, CH*H* Bn), 4.48 – 4.39 (m, 2H, C*H*H Bn, H-2), 4.35 (d, 1H, *J* = 12.0 Hz, CH*H* Bn), 4.02 – 3.99 (m, 2H, H-3, H-4), 3.67 (s, 3H, CH_3 CO_2Me); ^{13}C-APT NMR ($CDCl_3$, 101 MHz, HSQC): δ 170.5 (C=O), 137.4, 137.0, 133.5 (C_q), 132.1, 131.8, 129.1, 128.6, 128.5, 128.3, 128.2, 128.2, 128.1 (CH_{arom}), 88.5 (C-1), 79.9, 79.0 (C-3, C-4), 77.2 (C-2), 74.5, 72.8 (CH_2 Bn), 52.7 (CO_2Me); ^{19}F NMR ($CDCl_3$, 471 MHz): δ -68.03.

References and footnotes

(1) Richards, M. R.; Lowary, T. L. *ChemBioChem* **2009**, *10* (12), 1920–1938.
(2) Brennan, P. J.; Nikaido, H. *Annu. Rev. Biochem.* **1995**, *64* (1), 29–63.
(3) Lindberg, B. Components of Bacterial Polysaccharides. In *Advances in Carbohydrate Chemistry and Biochemistry*; Tipson, R. S., Horton, D., Eds.; Academic Press, 1990; Vol. 48, pp 279–318.
(4) Lowary, T. L. *Acc. Chem. Res.* **2016**, *49* (7), 1379–1388.
(5) Varki, A. *Glycobiology* **1993**, *3* (2), 97–130.
(6) Kinnaert, C.; Daugaard, M.; Nami, F.; Clausen, M. H. *Chem. Rev.* **2017**, *117* (17), 11337–11405.
(7) Shelton, J.; Lu, X.; Hollenbaugh, J. A.; Cho, J. H.; Amblard, F.; Schinazi, R. F. *Chem. Rev.* **2016**, *116* (23), 14379–14455.
(8) Altona, C.; Sundaralingam, M. *J. Am. Chem. Soc.* **1972**, *94* (23), 8205–8212.
(9) Taha, H. A.; Richards, M. R.; Lowary, T. L. *Chem. Rev.* **2013**, *113* (3), 1851–1876.
(10) Kilpatrick, J. E.; Pitzer, K. S.; Spitzer, R. *J. Am. Chem. Soc.* **1947**, *69* (10), 2483–2488.
(11) Altona, C.; Geise, H. J.; Romers, C. *Tetrahedron* **1968**, *24* (1), 13–32.
(12) Hagen, B.; van der Vorm, S.; Hansen, T.; Marel, V. D.; A, G.; Codée, J. D. C. Stereoselective Glycosylations – Additions to Oxocarbenium Ions. In *Selective Glycosylations: Synthetic Methods and Catalysts: Synthetic Methods and Catalysts*; Wiley-VCH Verlag GmbH & Co. KGaA, 2017; pp 1–28.
(13) Larsen, C. H.; Ridgway, B. H.; Shaw, J. T.; Smith, D. M.; Woerpel, K. A. *J. Am. Chem. Soc.* **2005**, *127* (31), 10879–10884.
(14) Smith, D. M.; Tran, M. B.; Woerpel, K. A. *J. Am. Chem. Soc.* **2003**, *125* (46), 14149–14152.
(15) Smith, D. M.; Woerpel, K. A. *Org. Biomol. Chem.* **2006**, *4* (7), 1195–1201.
(16) Tran, V. T.; Woerpel, K. A. *J. Org. Chem.* **2013**, *78* (13), 6609–6621.
(17) Larsen, C. H.; Ridgway, B. H.; Shaw, J. T.; Woerpel, K. A. *J. Am. Chem. Soc.* **1999**, *121* (51), 12208–12209.
(18) Shaw, J. T.; Woerpel, K. A. *Tetrahedron* **1999**, *55* (29), 8747–8756.
(19) Shaw, J. T.; Woerpel, K. A. *J. Org. Chem.* **1997**, *62* (20), 6706–6707.
(20) Bear, T. J.; Shaw, J. T.; Woerpel, K. A. *J. Org. Chem.* **2002**, *67* (7), 2056–2064.
(21) Codée, J. D. C.; Ali, A.; Overkleeft, H. S.; van der Marel, G. A. *Comptes Rendus Chim.* **2011**, *14*, 178–193.
(22) Green, L. G.; Ley, S. V.; Ernst, B.; Hart, G. W.; Sinaý, P. Protecting Groups: Effects on Reactivity, Glycosylation Stereoselectivity, and Coupling Efficiency. In *Carbohydrates in Chemistry and Biology*; Wiley-VCH Verlag GmbH, 2000; pp 427–448.
(23) Rhoad, J. S.; Cagg, B. A.; Carver, P. W. *J. Phys. Chem. A* **2010**, *114* (15), 5180–5186.
(24) van Rijssel, E. R.; van Delft, P.; Lodder, G.; Overkleeft, H. S.; van der Marel, G. A.; Filippov, D. V.; Codée, J. D. C. *Angew. Chem. Int. Ed.* **2014**, *53* (39), 10381–10385.
(25) van Rijssel, E. R.; van Delft, P.; van Marle, D. V.; Bijvoets, S. M.; Lodder, G.; Overkleeft, H. S.; van der Marel, G. A.; Filippov, D. V.; Codée, J. D. C. *J. Org. Chem.* **2015**, *80* (9), 4553–4565.
(26) To account for the difference in donor reactivity by the electron-withdrawing capacity of the functional groups at C2 and C5, the glycosylations were performed at a temperature adequate for conversion to the products (within four days), and were established prior to the generation of the data in Table 1.
(27) Napolitano, J. G.; Gavín, J. A.; García, C.; Norte, M.; Fernández, J. J.; Hernández Daranas, A. *Chem. – Eur. J. 17* (23), 6338–6347.
(28) Koźmiński, W.; Nanz, D. *J. Magn. Reson.* **1997**, *124* (2), 383–392.
(29) Marquez, B. L.; Gerwick, W. H.; Williamson, R. T. *Magn. Reson. Chem. 39* (9), 499–530.
(30) Gaussian 03, Revision E.01; **2004**, Gaussian, Inc., Wallingford CT.
(31) Ribeiro, R. F.; Marenich, A. V.; Cramer, C. J.; Truhlar, D. G. *J. Phys. Chem. B* **2011**, *115* (49), 14556–14562.
(32) The relative energies (in kcal·mol^{-1}) of the different oxocarbenium ions are, for the tribenzyl structures: ribo 0.0, arabino 0.1, lyxo 0.2, xylo 0.9; for the 2-fluoro structures: ribo 0.0, lyxo 0.9, ara 1.1, xylo 1.5; for the 2-azido structures: ribo 0.0, ara 0.6, xylo 1.3, lyxo 1.7; for the uronic acids: lyxo 0.0, ara 0.5, xylo 0.6, ribo 1.2.
(33) van der Heden van Noort, G. J.; Overkleeft, H. S.; van der Marel, G. A.; Filippov, D. V. *Org. Lett.* **2011**, *13* (11), 2920–2923.
(34) Mukaiyama, T.; Kobayashi, S. *Carbohydr. Res.* **1987**, *171* (1), 81–87.
(35) Doboszewski, B. *Nucleosides Nucleotides Nucleic Acids* **2009**, *28* (10), 875–901.
(36) Zhang, J.; Yuan, W.; Ma, X.; Wang, H.; Shao, H. *Chin. J. Chem.* **2014**, *32* (4), 361–364.
(37) Kakefuda, A.; Shuto, S.; Nagahata, T.; Seki, J.; Sasaki, T.; Matsuda, A. *Tetrahedron* **1994**, *50* (34), 10167–10182.